UNDERSTANDING THE ROLE OF MAGNITUDE ESTIMATION IN NAVIGATION

Joshua William Gaddy Yudice

Graduate School of
Systemic Neurosciences
LMU Munich

Dissertation at the
Graduate School of Systemic Neurosciences
Ludwig-Maximilians-Universität München

August 2022

Supervisor:
Prof. Dr.-Ing. Stefan Glasauer
Fachgebiet Computational Neuroscience
Brandenburg Technischer Universität Cottbus-Senftenberg

First Reviewer: **Prof. Dr. -Ing. Stefan Glasauer**
Second Reviewer: **Prof. Dr. Adreas Herz**
Third Reviewer: **Prof. Dr. -Med. Christian Sorg**
External Reviewer: **Prof. Dr. -Rer. Nat. Jan Wiener**

Date of Submission: August 3rd, 2022
Date of Defense: March 1st, 2023

Table of Contents

Summary

The purpose of this thesis is to describe how magnitude estimation enables path integration, which in turn provides a foundation for human navigation as a whole. This will be done over the course of four chapters, which are written to provide essential background concepts for two unpublished experiments conducted by the author.

The first chapter will introduce the cognitive process known as path integration and explain a probabilistic approach to modeling its function. It will also clarify the essential role of Bayes' Theorem and how we use modeling in the manuscripts to come.

In Chapter 2, we introduce how Bayes' theorem can be applied to the field of multimodal integration and, through the first manuscript, demonstrate how humans may combine optic flow with vestibular input when measuring angle.

In the third chapter, we will extend the previously used Bayesian models to investigate how the biasing influence of Bayesian priors can differentiate between applied navigation strategies.

Lastly, in Chapter 4 we will discuss the results from the two manuscripts, their interactions between each other, and what implications the results may have on our general understanding of navigation.

PREFACE

If someone were to have asked me about navigation, before I became scientifically involved in the topic, my first thoughts would have inevitably involved western society's historic journeys of exploration. I grew up with stories of the Oregon Trail, where countless souls adventured into the unknown wilderness of the now United States. Every day would have been a new environment, every landmark strange and devoid of context. In my fantasy, the only tools they had to guide themselves were the heavens, their memories, and the logical turnings of their mind. It was a story full of danger and excitement. However, most navigation that people do is significantly more mundane. To quote anthropologist Thomas Widlok, "They do not aspire to colonize the world and occupy places they've never visited. They are mobile but they are mobile in a restricted sense, they stay within a more or less defined cosmos., They are not going into unchartered territory. They are doing something quite different." (O'Connor, 2019).

When I did start researching navigation as a Master's Student, I was focused on this dichotomy between familiar and foreign environments. For me, the latter represented a difficult and interesting navigational problem, whereas the former was an easy and trivial every-day task. In a familiar environment, mostly people follow oft-practiced routes to get to their destinations. People would also know many landmarks with established spatial relationships between them that would allow them to easily improvise novel paths. Whereas in a foreign environment, the navigation-relevant information is comparatively sparse. Even if one has a vague idea of the destination, they need to closely monitor how far they have walked and in which direction, so they can methodically approach their destination. This process of combining orientation and distance estimates to determine position is often called "path integration", and although it is central to the more difficult problem of navigating unfamiliar environments, I would later find out that path integration is a fundamental process likely be involved in all navigation tasks.

CHAPTER 1: Introduction

Path Integration

Some of the most well-known experiments on path integration were conducted on Saharan Desert Ants. The ants could reliably execute straight return paths to their home location after heavily circuitous outbound paths without being able to see their nest. Researchers revealed that the ants were integrating the distance traveled as measured by number of steps (Wittlinger et al., 2007), and their orientation in space using primarily the polarization of the surrounding light (Muller & Wehner, 1988). We know now that path integration is a ubiquitous skill in the animal kingdom (for an overview, see Shettleworth, 2010). A diverse array of animals have been shown to use PI including, but certainly not limited to: crabs, ants, honeybees, spiders, gerbils, mice, bats, birds, monkey, and humans (Aharon et al., 2017; Collett, 2019; Fraser, 2006; Mittelstaedt & Mittelstaedt, 1982; Mittelstaedt & Glasauer, 1991; Moller & Görner, 1994; Muller & Wehner, 1988; Zeil & Layne, 2002). Naturally, among this exceptionally wide array of organisms is also a wide array of senses that can be used to execute PI. For example in crustaceans, hydrostatic pressure receptors are used to estimate angular rotations (Fraser, 2006) and in mice the airflow past their whiskers can provide information about displacement (Savelli & Knierim, 2019). Based solely on the wide-spread adoption of path integration as a solution to navigating, it is clearly a beneficial strategy in an evolutionary context, though we cannot know how ancient the ability might be.

In navigation research, path integration can be further subdivided into *allothetic* and *idiothetic* subtypes based on the information used to estimate orientation and distance. In *idiothetic* path integration (iPI), the navigator only uses self-motion information, which is sensory information produced because of the organism's movement. In humans, this includes cues from internal sources, like the vestibular organ, proprioceptive pathways, and efference copies of motor commands. It also includes cues from external sources like optic flow, which is the movement of the visual scene across the retina due to self-motion. In *allothetic* PI (aPI), the navigator also uses the location of external landmarks like the sun, a specific star, or another distant object to further inform calculations. Due to noise accumulation, self-motion information alone is not sufficient to accurately estimate one's position (Cheung & Vickerstaff, 2010) and, perhaps as a result, organisms always use allothetic PI if possible (Collett & Collett, 2000). In fact, the author is not

aware of any naturalistic situation during which an organism relies exclusively on iPI. What is therefore often done in order to study iPI in isolation, is to deprive the organism of all sensory information that might enable aPI (Fujita et al., 1990; Glasauer et al., 2002; Loomis et al., 1993; Wiener et al., 2010; Worchel, 1951).

Sidebar: Allocentric vs. Egocentric Navigation

The well-established sub-types of navigation called allocentric and egocentric navigation relate to the categorization of path integration into allothetic and idiothetic PI, and therefore deserve some background.

Allocentric navigation involves a map-like representation of space where objects and locations are defined relative to each other. This form of navigation is independent of the individual's current location or orientation. It is akin to viewing a map where you can understand the 'spatial relationships between different landmarks, regardless of where you are on that map. This type of spatial representation is crucial for understanding complex environments and complex navigation behaviors like making shortcuts. For example, when you navigate a city using a map, you are relying on allocentric representations to understand how different streets and landmarks relate to each other, irrespective of your current position (Klatzky, 1998).

On the other hand, egocentric navigation is centered around the individual's perspective. In this form of navigation, objects and locations are defined relative to the individual's current position and orientation. It is like navigating based on what you see in front of you, where spatial relationships are understood in terms of your immediate surroundings. This type of navigation is crucial for immediate, short-term movements and actions. For instance, when walking a familiar path through a city and you know which direction to turn at each intersection based on your orientation when entering each intersection (Klatzky, 1998).

The interplay between allocentric and egocentric navigation is a subject of ongoing research. Studies have shown that these two systems are not mutually exclusive but rather work together to facilitate effective navigation. For example, while navigating a familiar environment, you might switch between an allocentric view (understanding the layout of the environment as a whole) and an egocentric view (navigating through immediate obstacles) (Gramann et al., 2010).

Interestingly, the preference for allocentric or egocentric navigation can vary among individuals and can be influenced by various factors, including age and cognitive abilities. Research has shown that while some individuals may predominantly rely on an allocentric strategy, others may prefer an egocentric approach. This variability can have implications for understanding spatial cognition in different populations, including in the context of aging and neurodegenerative diseases (Colombo et al., 2017).

In summary, allocentric and egocentric navigation represent two fundamental ways in which space is perceived and navigated. Understanding the interplay between these two types of spatial representations is crucial for a comprehensive understanding of navigation and spatial cognition.

A foundational framework

As opposed to being a capability which is conditionally applied based on the navigational problem at hand, humans perform path integration automatically during all movements, regardless of task relevance (May & Klatzky, 2000). Work with model organisms, specifically ants, suggest that such a constant estimation of position may provide a spatial framework for memorizing landmarks (Müller & Wehner, 2010), which would be immensely helpful in unfamiliar environments. Further evidence from

insects suggest that the use of path integration in familiar environments is still helpful in that it allows the navigator to tolerate changes made to known landmarks (M. Collett & Collett, 2000).

In additional to experimental evidence, there are evidenced-based theoretical systems which outline how path integration could be used to construct map-like representations of complex spaces (Biegler, 2000; Wang, 2016). In 2000, Robert Biegler published a well-supported theoretical description of how path integration could support navigation at varying levels of complexity, from simple homing to a system that could "provide [a] unified, internally consistent, metric representation [of space]." In his paper, a "path integrator" functions as an accumulator which can be reset upon reaching a goal location. Although homing can be explained by a single integrator with one goal, which is also the reset location, he posits that a path integrator with multiple goals and resetting locations would be ideally suited to creating cognitive maps. His argument is supported by evidence from model organisms, showing that rats and gerbils can remember multiple destinations while performing path integration and that they have been shown to reset path integration at multiple locations (Gothard et al., 1996; Griffin & Etienne, 1998). A simple example of one variant he presented would be if the navigator performed path integration from one landmark to another, thereby establishing a spatial relationship between the two, and then reset their integrator in preparation for the next exploration.

Taking measurements

A prerequisite for path integration is the ability to accurately measure distances and angles. The first manuscripts presented in this Thesis will focus on two of the human senses required for idiothetic path integration (iPI) and the second manuscript will investigate iPI more holistically. Thus, in this section, I will outline the relevant types of self-motion information and describe the senses we use to measure them.

The main types of sensory information used by humans during iPI are vestibular input, optic flow, and proprioception. Additionally, though not sensory in origin, efference copies from the motor cortex can also provide useful information regarding self-motion. The vestibular organ can measure both linear and angular accelerations using the otolith organs and the semicircular canals, respectively. Since, they are only sensitive to acceleration, then moving at constant velocity will not be differentiable from being stationary (Bear et al., 2007). Optic flow on the other hand (the

movement of the visual environment through our field of view) can provide information about acceleration and velocity, including the direction of movement (Redlick et al., 2001). Proprioception is mediated by mechanosensory neurons in the muscles, tendons, and joints and provides us with information concerning the movement and position of our body parts (Tuthill & Azim, 2018). Lastly, the outgoing signals from the motor cortex controlling movement can be received by other parts of the brain, and this is called an "efference copy." The three previously listed senses accumulate noise inherent to producing the movement and sensing the movement, but the efference copy more directly reflects the intended action of a person. The role of efferent copies in human iPI is difficult to isolate, but research in rats has shown that disrupting both efference copies and proprioception has a profound impact on the rats' ability to perform directional path integration; more so even than removing visual cues (Stackman et al., 2003). Although it is clear that these 4 sources of information are all involved in iPI, the relative contributions to the process of path integration are still being researched.

Sidebar: Path Integration vs. Dead Reckoning

Historically, *Dead reckoning* is a traditional navigation method, particularly significant in maritime contexts. It involves estimating one's current position by starting from a known position and then applying knowledge of speed, time, and direction. This method is heavily reliant on external references, known as "fixes," which serve as crucial references in correcting accumulated errors and ensuring accurate navigation. In the absence of modern tools like GPS, dead reckoning was indispensable for maritime travel, with navigators using celestial bodies, landmarks, and later, chronometers and compasses to determine their position and course (Bennett, 2017).

The explicit nature of these calculations is what primarily distinguishes dead reckoning from path integration. The process is methodical and often involves tools and instruments to aid in these calculations, ensuring accuracy in navigation. While it can also use information about the external environment, *path integration* primarily occurs as an implicit process within neurological systems. It is a navigation strategy where an individual or animal internally updates its position relative to a starting location by integrating the distances and directions traveled. This process is less about explicit calculations and more about an innate, continuous updating mechanism within the brain (Etienne & Jeffery, 2004).

There are some interesting commonalities between the two concepts despite their differences. Both dead reckoning and path integration require a starting point and orientation to provide relevant information, they both involve the integration of self-movement information, whether it be about a ship or an organism, and they also share the challenge of accumulating errors over time. In dead reckoning, errors can arise from inaccurate measurements or changes in conditions, while in path integration, drifts in the internal sense of direction or distance can lead to inaccuracies (Cheung et al., 2007). In some ways dead reckoning seems to be a human invention that mirrors the biological process that is path integration.

Probabilistic representation of measurements

One complication involved in taking measurements is that the noise resulting from the sensory organs (measurement noise), neural

computations (system noise), and movements (motor noise) increase the variability of sensory measurements. If a person is asked to measure the same value 100 times consecutively, they will make different measurements over time due to the noisiness of their sensory organs. Similarly, if you ask a person to kick a ball at the same spot 100 times, the ball will land in a variety of locations due in part to motor noise. Since the vestibular system, vision, and proprioception all measure self-motion and we must first generate self-motion, then both sources of noise interfere with our measurements. With regards to path integration specifically, recent research has demonstrated that not only is noise present while executing planned paths (Chrastil & Warren, 2017), there is substantial noise during the encoding of distance and angle (Chrastil et al., 2019). Another study on the growing contribution of noise with age showed that the majority of noise present during PI originates during measurement of velocity, rather than integrating the measurements (Stangl et al., 2020).

Researchers who seek to better understand the cognition behind PI by using computational models represent a measurement not as a single value, but as a distribution of probable values. In this way, the noise or uncertainly regarding a sensory measurement can be quantified and propagated through the model. Often the distribution is normal, and the width of the distribution reflects uncertainty. As an example, imagine you are preparing to shoot an arrow at a target 10 meters away. In situations where measurement noise is low, e.g. assessing the distance to the target on a sunny day, then we would expect to see a narrower distribution of probable measurements. On the other hand, if we attempt to estimate distance in near darkness then we would expect to see a much wider distribution of probable measurements.

Formally speaking, this distribution is called a *likelihood distribution*. In the archery example, it is the probability of our current sensory measurement of distance, d, given that we are measuring distance to the target, D. This can be written as the conditional probability: $P(d|D)$. But in order to hit the target with the arrow, we do not want to know the probability of our measurement, we want to know the probability of the actual distance D, i.e. 10 meters. Thus, we need to compute the probability of the true distance, D, given our sensory measurement, d: $P(D|d)$.

Bayesian inference

This latter conditional probability, P(D|d), is called the *posterior distribution* in Bayes' theory and can be computed by considering both the current estimate of distance and previously accumulated information about the distance to the target. In our specific example, assume we have shot arrows from this same spot many times before. We have therefore repeatedly measured the distance and shot our arrows based on predictions of the distance. Assuming only that our predictions are noisy and not biased, the average of our prior predictions would eventually converge to the true distance D. After enough time we would attain a probability distribution for this context, i.e. this distance from the target: P(D). We call this the *prior distribution* and along with the probability of our immediate sensory measurement P(d), we can compute the posterior distribution:

$$P(D|d) = \frac{P(d|D) * P(D)}{P(d)} \tag{1}$$

The derivation of the above equation is based on the equality of $P(d \cap D)$ and $P(D \cap d)$, which are both the probability of the true distance and current distance being true, i.e. that our current distance matches the true distance.

$$P(d|D) \triangleq \frac{P(d \cap D)}{P(D)} \qquad P(D|d) \triangleq \frac{P(D \cap d)}{P(d)}$$

$$P(D \cap d) = \frac{P(d|D)}{P(D)} = \frac{P(D|d)}{P(d)}$$

In the context of behavioral neuroscience, we can use equation 1 to model a person's internal estimates of real-world values. This is exceedingly powerful because it allows us to quantify unmeasurable representations in the human brain. Of course, this assumes that a Bayesian model's predictions actually match human behavior and luckily research has shown that this is very often true of human perception and movement (Rescorla, 2021). In terms of measuring or estimating real-world magnitudes like distance and angle, Bayesian models can successfully explain behavioral effects like the central tendency effect, range effect, scalar variability, and sequential effects (Petzschner et al., 2015).

The Bayesian prior and the Central Tendency of Judgement

There is a ubiquitous and regularly documented behavioral effect characterized by the underestimation of large magnitudes and overestimation of small magnitudes when experimental subjects attempt to reproduce those magnitudes. This biasing of estimations toward the mean magnitude has been called the "Central Tendency of Judgement" (Hollingworth, 1910), "Central Tendency Bias" (Olkkonen et al., 2014), "Regression to the Mean" (Glasauer et al., 1995; Kaliuzhna et al., 2015; Loomis et al., 1993), as well as simply "Regression Effect"(Petzschner et al., 2015; Stevens & Greenbaum, 1966). It is well established that changing the range of stimulus magnitudes or their average size both impact the size of the bias, and more recent insights have shown that the order of stimuli probably plays a pivotal role in the size of the bias (Glasauer & Shi, 2021).

Early studies were primarily focused on documenting and manipulating the effect, but recent work has been focused on understanding the cognition that leads to the effect. One approach has been to model magnitude estimation data with computational models built on hypothesis about cognition. The Bayesian variety of these models have proven to be quite successful, suggesting the relevant cognitive process might be Bayesian in nature (see Glasauer & Shi, 2021 for review). In a Bayesian context, the Regression Effect is caused by the bias of the Bayesian prior on estimations of the magnitude stimulus. More specifically, when the prior distribution is integrated with the likelihood distribution, the mean of the resulting posterior is an intermediate value between the means of the prior and likelihood. Since the mean of the likelihood approximates the observed stimulus and the mean of the prior distribution eventually converges to the mean of all experienced magnitude stimuli, then over many trials, the consistent bias of the prior on the posterior produces the Regression Effect.

One aspect of the likelihood distribution that contributes to its plausibility is that it represents the uncertainty of sensory measurements, and that our internal representation of the true real-world value is not the same as the true value. The biological transformation of the true stimulus into an internal representation is included in some Bayesian models, including the two-stage Bayesian estimator model that will be described later. Similarly, the Bayesian prior distribution is stored as an internal representation and is also not strictly bound to the true stimulus values. What this means, is that the biasing effects of the prior can produce the Regression Effect as it is classically defined, but might not always.

This can be demonstrated by disrupting the cognitive processes of calibration and adaptation. As an example, let us take a visuomotor adaptation experiment like the one originally conducted by Von Helmholz in 1867 (Helmholtz, 1867). In this study, participants were instructed to reach towards specific targets while their vision was altered by prism glasses, causing a lateral shift in their field of view. Initially, when the visual shift was towards the left, participants tended to overshoot the target in the same direction. However, with practice, they adjusted to the altered visual input. This adjustment process is often called "recalibration" or "adaptation" of their sensorimotor system. Interestingly, Helmholtz noted that upon removal of the prism glasses, participants' attempts to reach the targets inaccurately veered to the right, a phenomenon referred to as the after-effect of adaptation. Recalibration is made possible by the feedback loop between initiated motor commands and visual feedback concerning the outcome.

Now imagine we remove the feedback, perhaps by blocking vision directly after the participant initiates the motor command. A constant disparity between the true stimulus values and the internal representation would remain throughout the experiment since recalibration would not be possible. In the data, we would still likely see overestimation of small stimuli and underestimation of large stimuli, but the global over- or underestimation of all stimuli would be there too (Figure 1). The combination of a centralizing bias with a constant underestimation seen in the far-right plot of Figure 1, does not conform to the classic definition of the Regression Effect. If we define the Regression Effect as the biasing effect of the “mean stimulus” then the resulting data would not demonstrate a Regression Effect as per the original definition, since the mean of the prior is now different than the mean of the stimulus. This special case is relevant to this thesis because all experiments presented here were designed not to include feedback for participants, so we cannot assume that the mean of the prior distribution matches the mean of the stimulus distribution. Furthermore, it is possible that the size of the global over or underestimation would be different from one participant to another, due to individual differences in sensory processing, and these would not be corrected by calibration.

In conclusion, within this thesis and the manuscripts contained therein, we will refrain from using the classically defined terms listed in the first paragraph of this section. To assure a conceptual separation from the behavioral effect observed by Hollingworth in "The Central Tendency of

Judgement", we will refer to this more specific type of bias as the Prior's Centralizing Bias (or PCB). Furthermore, we will conceptually separate the PCB from a global shift in estimated magnitudes, since the latter is impacted by a lack of recalibration based on feedback. Lastly, we will often measure PCB as 1 minus the slope of the regression line in plots of stimuli versus estimations.

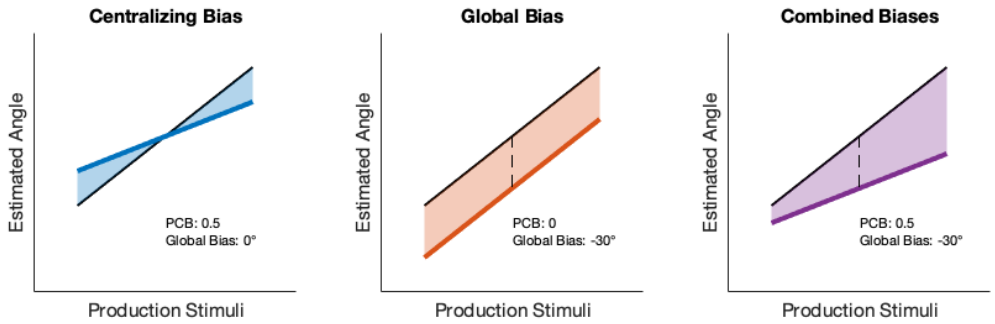

Figure 1: Disassociating Global Shift from the Centralizing Bias. In situations where sensorimotor recalibration is not possible, an experimenter might find a global bias in estimates of perceived magnitudes due to a mismatch between the pre-existing and actual stimuli ranges in the participants. In these cases, the centralizing bias of the prior distribution (first panel, termed Prior's Centralizing Bias, or PCB) on estimates would be dissociable from the global bias (second panel), but both would still be present in the data (see third panel for example of summed effect).

The PCB and the role of relative variance

For humans, conceiving of and representing the world is a continuous and recurrent process of measurement and estimation. If we can understand the influence of our prior experiences on our immediate estimations, we would be better prepared to understand how we perceive and act in the world, including how we navigate. In this section, we will look at how the noisiness of our sensory measurements in relationship to the noisiness of our own internal processing, impacts our estimations of measured magnitudes. In a Bayesian context, this relationship is that between the variance of the Likelihood distribution and the variance of the Prior, both of which are assumed to be Gaussian probability density functions and could therefore be represented as:

$$f(x|\mu,\sigma^2) \triangleq \frac{1}{\sqrt{2\pi\sigma^2}} e^{-\frac{(x-\mu)^2}{2\sigma^2}} \quad (2)$$

Using this equation as a foundation, we can calculate the mean of the Posterior distribution as follows:

$$\mu_C \triangleq \frac{\frac{\mu_A}{2\sigma_A^2} + \frac{\mu_B}{2\sigma_B^2}}{\frac{1}{2\sigma_A^2} + \frac{1}{2\sigma_B^2}} = \frac{\mu_A\sigma_B^2 + \mu_B\sigma_A^2}{\sigma_B^2 + \sigma_A^2} = \frac{\sigma_B^2}{\sigma_B^2 + \sigma_A^2} * \mu_A + \frac{\sigma_A^2}{\sigma_B^2 + \sigma_A^2} * \mu_B \quad (3)$$

$$\mu_C = w_A * \mu_A + w_B * \mu_B \quad (4)$$

In this formulation, we can see how means of the component distributions are summed, and the weighting of the summation is determined by the relative variances of each distribution. Since it is not intuitive that the weight of mean A is determined by standard deviation of B, let us reorganize the variables.

$$w_A = \frac{\sigma_B^2}{\sigma_B^2 + \sigma_A^2} = \frac{\frac{1}{\sigma_A^2}}{\frac{1}{\sigma_A^2} + \frac{1}{\sigma_B^2}} \quad e.g. w_{likelihood} = \frac{\frac{1}{\sigma_{likelihood}^2}}{\frac{1}{\sigma_{likelihood}^2} + \frac{1}{\sigma_{prior}^2}} \quad (5)$$

Now we see how the weight, for example, of the likelihood's mean to the mean of the posterior distribution is related to the variances of the prior and likelihood. Namely, the greater the variance of the likelihood in comparison to the prior, the less its mean contributes to the mean of the posterior distribution. This is intuitive since measurements that have low variance are more consistent and reliable and should contribute more to our final estimate.

If we were to experimentally manipulate the variability or noisiness of sensory stimuli, thereby increasing the variance of the associated likelihood distribution, we should see a proportional increase in the biasing effects of the prior on people's estimates. In 2014 Olkkonen et al. demonstrated this exact outcome in the context of color perception by adding chromatic noise to their color stimuli (Olkkonen et al., 2014). In doing so, they saw a clear increase in the Regression Effect with added noise. This relationship between likelihood variance and the Regression Effect has also been demonstrated in the context of length comparison, where the variance of the likelihood was assumed to increase with elapsed time after the stimulus was experienced

(Ashourian & Loewenstein, 2011). Thus, by looking at the Regression Effect, or more specifically the PCB, we can gain valuable insight into how much the prior is relied upon in a given context.

The two-stage Bayesian estimator model

In this section, let us consider how the treatment of Bayesian priors can differentiate between models. One approach is to assign a fixed mean and variance to the prior distribution based on the characteristics of the stimulus distribution (Cicchini et al., 2012; Jazayeri & Shadlen, 2010). This assumes that the participants know the distribution of stimuli before experiencing them. Another approach is to include a rule for updating the prior based on predictions so that after every prediction the mean and variance of the prior will change. In this case, it is still necessary to make an assumption at trial one, however the model will learn the stimulus distribution over time much like a person would. Furthermore, with this type of model it is possible to predict sequential trial effects, which are how recent stimuli affect predictions of the current stimulus through modifying the prior, and range effects, which are how the strength of the PCB grows with mean stimulus size (Glasauer, 2019; Petzschner et al., 2015). The model utilized in the following manuscripts takes the latter approach and is therefore capable of predicting nuanced behavior despite having very few free parameters. Since the Bayesian models are core features of both manuscripts, let us take some time to examine the structure and the underlying assumptions of this model. (For justification and full mathematical formulation, please see Glasauer, 2019 and Petzschner & Glasauer, 2011)

Originally described by Petzschner and Glasauer in 2011, the "two-stage Bayesian estimator" model iteratively: 1) converts the incoming stimuli to a measurement on a logarithmic scale, 2) updates the prior distribution based on the likelihood distribution of said measurement, 3) integrates the likelihood with the prior to yield a posterior distribution, and 4) converts the posterior distribution back onto a linear-scale before 5) selecting a value as a response. Within the logarithmic space where Bayesian integration happens, all probability distributions are assumed to be normal, which means that the final posterior-distribution on a linear-scale is log-normal.

$$\mu_{likelihood} = \ln\left(1 + \frac{d_m}{d_0}\right) + n_m \qquad (6)$$

The 2-stage Bayesian model converts the incoming measurement of the stimuli (d_m) into the logarithmic scale because it mirrors the well-established Weber–Fechner principle, which asserts that perception scales logarithmically with stimulus intensity; a notion first put forth by Gustav Fechner. Recent psychophysical studies corroborate this, demonstrating that human estimations of numerosity (Dehaene et al., 2008), angular velocity (Jürgens & Becker, 2006), and locomotor distance(Durgin et al., 2009) usually adhere to this logarithmic pattern. Consequently, the model incorporates this logarithmic transformation in a way that is comparable to the methodology used in modeling speed discrimination behavior published by Stocker & Simoncelli in 2006 (Stocker & Simoncelli, 2006). Within the log function, 1 is added to accommodate measurements of 0, and the measurements are dividing by a scaling variable (d_o) which can be used to adjust the "flatness" of the log-function. Additional sensory noise (n_m) associated with the measurement of the stimuli can be included if desired.

The model does not explicitly maintain the variance of each distribution. Instead, when combining distributions, e.g. A and B, the mean of the product distribution is calculated via weighted summation of the means of A and B (Laming, 1999). As seen in equation 3, the weights during this summation reflect the ratio of the variances of distributions A and B. Since the ratios of variances in equation 3 are compliments of each other:

$$1 - \frac{\frac{1}{\sigma_B^2}}{\frac{1}{\sigma_A^2} + \frac{1}{\sigma_B^2}} = \frac{\frac{1}{\sigma_A^2}}{\frac{1}{\sigma_A^2} + \frac{1}{\sigma_B^2}} \tag{7}$$

we can rewrite equation 4 to be the following:

$$\mu_C = w_A * \mu_A + (1 - w_A) * \mu_B \tag{8}$$

This way, only one weight needs to be calculated to determine the mean of distribution C. There are 2 weights like this in the 2-stage Bayesian model, corresponding the 2-stages: one for updating the prior based on the likelihood and another for computing the posterior distribution from the likelihood and prior. The calculation of means in these two situations, respectively, are:

$$\mu_{prior} = w_1 * \mu_{prior} + (1 - w_1) * \mu_{likelihood} \tag{9}$$

$$\mu_{posterior} = w_2 * \mu_{prior} + (1 - w_2) * \mu_{likelihood} \quad (10)$$

In practice, both weights are derived from a single fitted parameter according to a 1-dimentional derivation of the Kalman filter. This fitted parameter is the ratio of measurement noise (variance of the likelihood) to system noise (variance during updating). In basing both weights on the same fitted parameter, the model creates an interaction between the influence of the prior during posterior calculation and during prior update. Specifically, as measurement noise increases (in relationship to system noise), the prior is weighted less when calculating the posterior and when updating the prior (Figure 2).

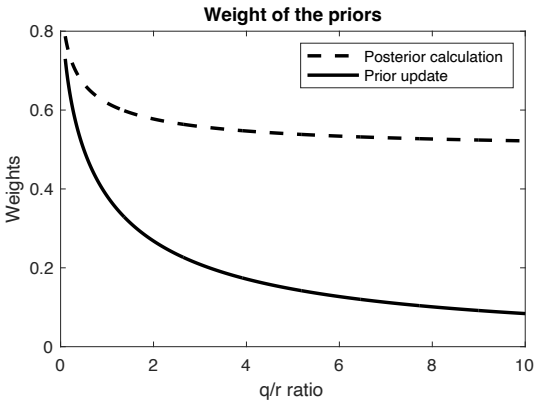

Figure 2: The weight of the prior as a function of system noise over measurement noise (q/r). As q/r grows, the weight of the prior decreases during prior update and during the calculation of the posterior. The lower limit on the weight of the prior during calculation of the posterior is 0.5, meaning the likelihood is always weighted equally or more than the prior.

This is intuitive since an unreliable measurement (high variance of the likelihood) should bias our internal estimates less and contribute less to our final responses. One important feature here, is that the weight of the prior during posterior calculation can be no less than 0.5, meaning that the likelihood always contributes to the posterior equally or more than the prior.

The model as a whole only has 2 free parameters, and the second one determines how the prediction is selected from the posterior distribution. Before the posterior is transformed back to a linear scale (the reverse process of equation 6), the model adds a fitted shift to the mean of the posterior distribution.

$$d_r = e^{\mu_{post} + \Delta x} * d_0 \quad (11)$$

The terms here are the selected response (d_r), arbitrary scaling constant (d_0), mean of the posterior (μ_{post}) and the shift parameter (Δx). The shift parameter is necessary since, unlike a normal distribution, the final log-normal posterior distribution has a different mean, median, and mode. Rather than assuming which value is appropriate in all cases, the model fits the shift parameter for each training data set. Changes to the shift parameter can lead to a general over or underestimation of the model's responses.

One final point for consideration are the assumptions associated with evaluating the model over experimental data. As is standard, the free parameters of the model will be fit in one experimental condition and evaluated in another. As long as the context of the conditions remains constant, in terms of the sensory input and task requirements, we assume that the fitted parameters will be appropriate in both conditions.

In summary, the described model assumes that:

1) our sensory representation of a magnitude is dependent on the real-world value.
2) during the first measurement, the mean of the prior equals the measurement.
3) Bayesian Integration takes place in a logarithmic scale.
4) all probabilistic distributions directly involved in Bayesian integration are normal.
5) the ratio of measurement noise and system noise is constant within a stable context.
6) the tendency to over- or underestimate is constant within a stable context.
7) motor noise will not cause a systematic bias of responses.

The two-stage Bayesian estimator model is both efficient in its use of free parameters and efficacious in predicting human responses. The variations on this model presented in the following manuscripts will represent competing hypotheses and their success relative to each other will resolve open questions in the fields of magnitude estimation and navigation.

Improving noisy measurements

As previously stated, when discussing the use of likelihood distributions, there is noise during sensory processing and neural integration which leads to more variability in our measurements and actions. We can mitigate measurement noise to some extent by taking redundant measurements of the same quantity. A good example of this is source localization: let us say you are one a hike in the woods and something moves in the bushes next to you. By combining the auditory and visual senses, you could locate the cause more quickly than using either alone (Vilares & Kording, 2011). This area of research is called multi-modal integration and is especially relevant to path integration because our senses for self-motion are very redundant. When we perform a whole-body rotation, our semicircular canals register the angular acceleration, optic-flow provides a visual cue that we are turning, proprioceptive information tells us about our postural changes involved in turning, and we receive efference copies of the motor command to turn. It seems intuitive that measuring the same quantity in multiple ways would increase the precision of our measurement, but this idea has also been formalized using Bayesian statistics (Ernst & Banks, 2002; Ernst & Bülthoff, 2004; Landy et al., 1995).

Let us return our attention to equations 3 through 5. So far, we have applied these equations when integrating the likelihood and prior distributions, but the same equations can be applied to integrating two likelihood distributions as well. What was not shown earlier is how to calculate the variance of the resulting distribution:

$$\frac{1}{\sigma_C^2} \triangleq \frac{1}{\sigma_A^2} + \frac{1}{\sigma_B^2} \tag{12}$$

$$\sigma_C^2 = \frac{1}{\frac{1}{\sigma_A^2} + \frac{1}{\sigma_B^2}} = \frac{1}{\frac{{\sigma_B}^2}{{\sigma_A}^2{\sigma_B}^2} + \frac{{\sigma_A}^2}{{\sigma_A}^2{\sigma_B}^2}} = \frac{{\sigma_A}^2{\sigma_B}^2}{{\sigma_A}^2 + {\sigma_B}^2} \tag{13}$$

Interestingly, the variance of the resulting distribution is less than or equal to the variance of either contributing distribution. As an example, this means that if we combine the likelihood distributions associated with visual and

vestibular sensory measurements, the resulting multimodal likelihood distribution would have an equal or lesser variance then either.

If we consider this fact in the context of calculating the posterior mean via a weighting sum (equation 4), we can see that a multimodal likelihood would have a weight equal to or less than the likelihood of either visual or vestibular senses alone:

$$w_{priorC} \leq min(w_{priorA}, w_{priorB}) \tag{14}$$

Weighting the prior less and the likelihood more over many trials would lead to a smaller PCB and overall, more accurate estimations of magnitudes. Thus, we have a formal Bayesian mechanism for calculating how multimodal integration results in more accurate estimations overall.

Individual differences when measuring rotation

Another interpretation of the width of the likelihood distribution is as a measure of the trustworthiness or reliability of a sensory input. When measuring one value, an ideal sensory organ would always provide the same measurement. So a wide distribution, which indicates highly variable sensory inputs, would not be reliable. This inverse relationship between variance and reliability is included in equations 4 & 5, where we can see that a larger variability (standard deviation) leads to a lower weighting when determining the multimodal mean.

It has been shown that experimentally modulating the reliability of a sense impacts its influence on perception and in many cases the degree of this effect can be explained by Bayesian MLE (Alais & Burr, 2004; Battaglia et al., 2003; Ernst & Banks, 2002; Kaliuzhna et al., 2015; Prsa et al., 2012). A sense's reliability can also be altered via a pathology. For example patients who have had Vestibular Neuritis often rely more on their visual input afterwards due to damage of their vestibular nerve (Cousins et al., 2014).

Similarly, variability in age, genetics, and life experience will lead to differences in the acuity of vision, hearing, and vestibular function that would inevitably influence inter-modality weightings. It has also been shown that the ability to integrate multisensory information is limited in children and matures over the course of one's life, being molded extensively by experience (Murray et al., 2016). Thus, when performing experiments on

multi-modal integration, one would expect to see variable inter-modal weightings among participants.

Sidebar: Circular Data and Statistics

Circular or periodic data is a fascinating type of data that stands apart from traditional linear data due to its *bounded* and *cyclical* nature. This form of data is best understood through examples such as calendar years, time of day, and angles, each embodying the concept of periodicity. The end of one cycle seamlessly connects to the beginning of the next, creating a continuous loop. This characteristic poses distinct challenges and opportunities for analysis and interpretation.

For instance, in calendar years, December leads into January, forming a cycle that repeats annually. Similarly, the time of day cycles every 24 hours, with midnight flowing into the early hours of a new day. Angles, measured in degrees, also exhibit circularity; 360 degrees brings you back to 1 degree when rotating clockwise. Unlike linear statistics, where data points are spread along a straight line, circular statistics deal with data that wraps around a circle, presenting unique challenges and requiring different analytical approaches.

In linear statistics, the concept of average or mean is straightforward, but in circular statistics, calculating an average becomes more complex due to the *cyclical* nature of the data. For example, the average of 359 degrees and 1 degree isn't 180 degrees, but rather 0 degrees, illustrating the need for specialized methods in circular statistics. This same property also complicates the calculation of variance, i.e. how far data points are spread out from the mean. Variance also must account for the circularity, where two points close on the circle might be far in linear terms.

In terms of angles specifically, which are often used to represent periodic data, the application of circular statistics can be particularly relevant. When deciding if circular statistics is an appropriate choice for a data set, consider if 1, the data is inherently *bounded* within the limits of a circle; meaning that the values are constrained within a 0 to 360 degrees range. And 2, if the data is *cyclical*, mean that an angle of 370 degrees would instead be recorded as 10 degrees. These qualities of being both *bounded* and *cyclical* are good indicators that circular statistical methods may be appropriate.

Circular statistics can also be helpful when considering the directional nature of cyclical data. For example, when measuring turn angle, positive and negative values often denote different directions of rotation that can sometimes lead to the same final orientation. For example, a counterclockwise turn of -120 degrees would result in the same final orientation as a clockwise turn of +240 degrees (sign signifies directionally). This aspect is particularly relevant when evaluating hypotheses about orientation data but would be less relevant when evaluating hypotheses about the magnitude of the turn angles themselves as magnitudes are the absolute size of the angle. In cases such as the former, circular statistics would provide a more nuanced and accurate understanding of circular data than traditional linear statistical methods (Apuzen-Ito, 2014; Pewsey et al., 2013).

In the manuscripts included in this Thesis, we often analyze circular data, but we are always evaluating hypothesis about magnitudes, namely the absolute size of a turn's angle as opposed to the final orientation. These magnitudes are neither *bounded* nor *cyclical*, extending from 0 to positive infinity. Directionality is often represented by signed numerical values, but there are no cases in which the outcome of different turning angles is considered equivalent. Thus, linear statistical methods are used throughout.

Self-rotation perception using visual and vestibular stimuli relies on prior information and sensory fusion

Joshua W.G. Yudice[1], Johanna Bayer[4,5], Chris J. Bockisch[3], Juliane Pawlitzki[1], Zhuanghua Shi[2], Stefan Glasauer[1]

1. Computational Neuroscience, Brandenburg University of Technology Cottbus-Senftenberg, Platz der Deutschen Einheit 1, 03046 Cottbus, Germany

2. Allgemeine Psychologie, Department Psychologie, Ludwig-Maximilians-Universität München, Leopoldstr. 13, 80802 München

3. Department of Neurology, University Hospital Zurich, University of Zurich, CH-8091 Zurich, Switzerland

4. Orygen, The National Centre of Excellence in Youth Mental Health, 35 Poplar Road, Parkville VIC 3052, Australia

5. Centre for Youth Mental Health, The University of Melbourne, VIC, 3052, Australia

ABSTRACT

When humans sense self-rotation, vestibular and visual sensory information can be integrated to reduce sensory noise and provide more accurate and precise estimates of displacement than either modality alone. In this experiment, 18 healthy participants completed a production-reproduction task where they reproduced angular displacement. We found that on average reproduction was more accurate and precise in the bimodal condition, where both visual and vestibular information were available, than when only one sensory modality was available. We show that a systematic centralizing bias seen during self-rotation reproduction can be well explained by a Bayesian model which maintains a prior for angular displacement, and a Bayesian model assuming sensory fusion explains these biases better than models that use a single modality. Lastly, we showed that the Bayesian model assuming sensory fusion outperformed either unimodal model in explaining the bimodal condition data. Taken all together, these results demonstrate that our participants relied on prior information and fused sensory inputs according to Bayes' Theorem.

INTRODUCTION

People internally represent their position and orientation in their environment and automatically update this representation when they move (May & Klatzky, 2000). Essential to this process, termed path integration, is the ability to accurately measure angular displacement. When humans sense self-rotation, endolymph movement through the semicircular canals and movement of the visual environment over the retina (optic flow) provide measurements of angular velocity that can be used to compute angular displacement. However, sensory measurement of angular velocity is noisy and thus can lead to errors in perceptual estimates of self-displacement. When both vestibular and visual sensory information is available, they can be integrated to reduce sensory noise and provide more accurate and precise estimates of displacement than either modality alone (van Dam et al., 2014).

Previous research on multisensory integration has been able to successfully model a variety of behavior in humans and model organisms using Bayesian models that represent sensory measurements as probabilistic likelihood distributions (Alais & Burr, 2004; Ernst & Banks, 2002; Hillis et al., 2004; Jacobs, 1999; Jürgens & Becker, 2006; Knill & Saunders, 2003; Landy et al., 1995; van Beers et al., 1999, 2002). When all probabilistic distributions are Gaussian, then multiplying two unimodal likelihood distributions results in a multimodal likelihood distribution which has a lower variance than either unimodal likelihood distribution, thus providing a mechanism for the improved precision witnessed in multimodal contexts (Ernst & Bülthoff, 2004). Fusion of sensory inputs reliably occurs as long as both sensory measurements are presumed to be measuring the same thing (Kayser & Shams, 2015; Körding et al., 2007) and the measurements themselves are not hugely different (Jürgens & Becker, 2006). In the experiment presented here, participants are required to measure and reproduce whole-body yaw rotations, which they perceive through the visual and vestibular systems. The multimodal stimulus is very naturalistic, consisting of redundant (i.e. fully agreeing) visual and vestibular measurements of the participant's turn. Since the source is the same, i.e. the participant's perceived rotation, and the measurements agree, fusion was expected to occur.

The primary goal of this paper is to demonstrate that visual input and vestibular input generated by self-rotation are fused according to Bayes' Theorem. In order to prove this, we conducted an experiment in which participants reproduce experienced turns in 3 experimental conditions differentiated by the availability of sensory modes: only visual information, only vestibular

information, and both information-types available. Rhetorically, we will reach this conclusion in 3 steps: 1) demonstrate that our participants have benefits to precision and accuracy in the bimodal condition compared to either unimodal condition. 2) Show that a Bayesian model that assumes sensory fusion can predict the extent of systematic over/underestimations of the turn magnitudes. 3) The same Bayesian model can predict the participants' data in the multimodal condition better than a Bayesian model that assumes only one sense is used for the task.

The first step is to confirm that our participants demonstrate the benefits to precision and accuracy characteristic of sensory fusion. Accuracy refers to how closely reproductions of a turn match the true value and precision refers to the overall variability of reproductions. We expect reproductions to be the most accurate and precise in the bimodal condition because their multimodal representation of the turn angle is less variable, thanks to Bayesian integration, and this leads to reproductions that resemble the stimuli more closely. The second step is to determine if a probabilistic Bayesian model (replicated from Petzschner & Glasauer 2011) that assumes sensory fusion occurs can predict the bimodal condition data better than variants of the model that use only one sensory modality. To this end we will fit the Bayesian model to each unimodal condition to obtain a free parameter specific to each modality. We will mathematically calculate the bimodal version of this free parameter based on the unimodal values, and then use that calculated free parameter to predict the bimodal data. The success of predictions will be assessed via the Coefficient of Determination (R^2) as well as the similarity of systematic under/overestimations between behavioral data and model predictions. It is necessary to compare the unimodal variant of the model to the bimodal variant because we are interested in goodness-of-fit due to the assumed sensory fusion and not just the existence of a Bayesian prior.

METHODS

Participants

Twenty volunteers participated in the study without monetary compensation and two participants were excluded due to nausea in the visual condition. The final pool of participants (6 female, 12 male) had a mean age of 33.8 years and standard deviation of 10.8 years. All included participants had normal or corrected-to-normal vision and had little to no susceptibility to motion-induced nausea. A local ethics committee approved this experimental design in accordance with the Declaration of Helsinki.

Experimental setup

The experiment was conducted on a rotating chair positioned within a cylindrical drum that could rotate separately from the chair (fabricated by Toennies, see Figure 2A). Participants sat in the chair and were head-fixed such that they would spin around their head's central axis. The walls of the drum were approximately 74 cm from the participant's eyes and covered in vertical contrast bars 10 cm wide. No discernable landmarks were present aside from the repeating contrast bars and diffuse light was provided by a lamp positioned over the participants' heads. White noise was played over speakers to obscure the sounds of the machine. Participants controlled the reproduction movement of the chair using handheld buttons: one button for right-ward motion, one for leftward-motion, and one button to confirm selections. Movement in all directions was allowed until confirmation, which was followed by a 3-second pause and then the next trial.

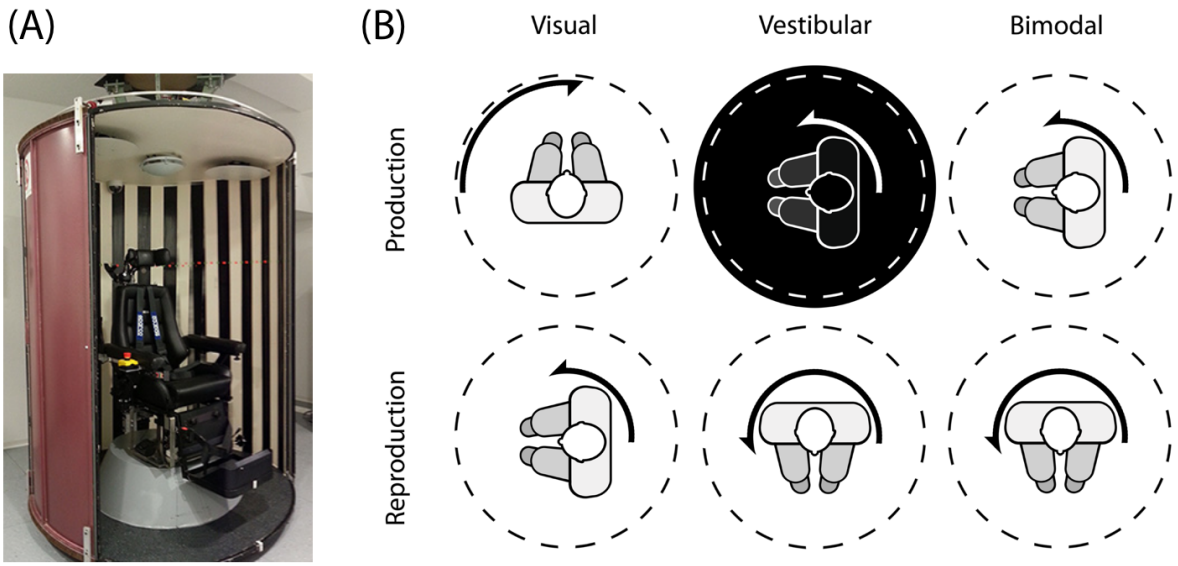

Figure 1. Experimental materials and procedure. **(A)** Photograph of the rotating chair and drum. Head was fixed and participants were secured using safety belts. Responses were made with handheld button boxes. **(B)** The experimental paradigm consisted of three conditions: Visual, Vestibular, and Bimodal. Each condition had two portions: production, in which either the drum or chair is rotated, and reproduction, in which the participant actively rotates the chair in the same direction and magnitude as the perceived production distance.

Experimental procedure

Ability to estimate angular distance was assessed using a production-reproduction task. During the production phase, participants passively experienced an angular displacement of the drum or chair and then had to actively reproduce the same distance in the same direction by rotating the chair using button presses. Reproductions were always bimodal regardless of condition, i.e. the drum was visible as the participant's rotated their chair via button presses Figure 2B).

Visual Condition. The production distance was provided by rotating the drum while the chair remained stationary. Movement of the contrast bars induced a feeling of self-motion in the direction opposite to drum rotation. To reproduce the distance, the participants were instructed to actively rotate the chair in the direction of perceived movement.

Vestibular Condition. The production movement consisted of passive rotation of the chair in darkness. The lights were switched on for reproduction and participants were instructed to replicate the movement in the same direction.

Bimodal Condition. Lights were on during both production and reproduction, such that participants had both visual and vestibular input during rotation. Production distances were provided by rotating the chair.

One hundred trials were presented for each condition. Distance stimuli consisted of 20 repetitions of 5 different angular distances (from 50° to 130°, at intervals of 20°), which were randomly permutated. The sequence of trials was held constant across participants so trial-wise effects would be comparable. To discourage the use of time estimation, movement velocity in the production phase was varied within ±60% of 25 degrees/second (scaling factor drawn from a truncated Gaussian distribution). Whereas the velocity during the reproduction phase was always 25 deg./sec.^{2}. The acceleration and

deacceleration in both phases was always 25°/sec^2. Each condition lasted between 23 and 27 minutes, depending on how quickly participants completed the reproduction movements.

Analysis of behavioral data

To reveal trends in accuracy and precision, the absolute behavioral error (absolute value of reproduction minus stimulus) and the standard deviation of errors, respectively, were calculated for each stimulus size for all participants and conditions. A 2-way analysis of variance (ANOVA) was performed for each metric using experimental condition and stimulus size as factors. One-tailed paired t-tests were also performed for both metrics to validate the hypothesis that both error and standard deviation is larger in the unimodal conditions than the bimodal conditions. Data analysis and modelling was performed using custom written Matlab (Mathworks, US) scripts.

We expected to observe a systematic error often made during magnitude estimation, which is a consistent overestimation of small turn angles and a consistent underestimation of large turn angles compared to the mean of all turn angles. This bias is referred to as the Regression to the Mean or the Central Tendency of Judgment (Hollingworth, 1910; Loomis et al., 1993; Olkkonen et al., 2014; Petzschner et al., 2015; Prsa et al., 2012), and constitutes an overestimation of small stimuli and an underestimation of large stimuli due to the biasing influence of the *mean or median of the stimulus range*. In all cases, the Regression to the Mean was calculated by plotting the production stimuli against the behavioral reproductions or model predictions, and then fitting a regression line to the data. The compliment of the slope of this line (1-slope) indicated the size of the Regression to the Mean. In this paper, we are more interested in the centralizing *bias of the Bayesian prior* on the reproductions, rather than the bias of the mean stimulus, so we will refer to the compliment of the slope as the Prior's Centralizing Bias (or PCB). It is important to differentiate this because we do not provide feedback to our participants concerning correctness of their reproductions, and therefore they cannot recalibrate their sensorimotor system to eliminate global errors affecting all reproductions (would appear as a vertical shift of the regression line in the aforementioned plot. We use the PCB as an indicator of both overall accuracy and how much a participant relies on their prior (Jazayeri & Shadlen, 2010; Petzschner & Glasauer, 2011; Roach et al., 2017). We conducted two one-tailed paired t-tests to confirm that we see a lower PCB in the bimodal condition (higher accuracy and lower reliance on a Bayesian prior) when compared to the unimodal conditions.

Linear statistics are applied for analyzing angular data here since we analyze only magnitudes and the differences between them. Since magnitudes do not exhibit the cyclical and bounded characteristics of circular data, but instead extend from 0 to positive infinity, linear statistical methods are appropriate. Regarding multiple comparisons, all hypothesis tests were grouped according to the assertions in the introduction or if a post-hoc question arose. Corrections of the significance threshold was done with the Holm-Bonferroni method.

Bayesian estimator models of bimodal integration

Unimodal Models

What we refer to as the Unimodal Model (UM) is entirely equivalent to the Petzschner & Glasauer 2011 two-stage model (Petzschner & Glasauer, 2011). This model iteratively processes the angular

distance stimuli in the same order as the participants experienced them. In a single iteration, the model works as follows:

1. The angle stimulus is transformed into log space, where we assume all involved probability distributions are Gaussian. The transformation is done to mirror the Weber–Fechner law; a practice which has been substantiated by related studies (Dehaene et al., 2008; Durgin et al., 2009; Jürgens & Becker, 2006) and has been previously applied with regards to speed discrimination (Stocker & Simoncelli, 2006).
2. The likelihood distribution (mean equal to the log-transformed stimulus value) is fused with the prior distribution (its mean is iteratively updated). To calculate the mean of the posterior distribution, a weighted sum of these two means is performed where the weights are determined by a single fitted parameter (r/q ratio), which represents the ratio of measurement noise (sensory noise, r) to process noise (noise during prior update, q).
3. The mean of the prior distribution is updated according to a weighted sum of the likelihood's mean and the mean of the prior from the preceding iteration. This weight is calculated using a Kalman filter (Kalman, 1960), which also relies on the r/q ratio. In the first iteration, the mean of the prior is assumed to be equal to the first measurement.
4. Finally, the model's prediction of the current reproduction is determined as the maximum (mode) of the posterior distribution plus a fitted constant, termed "shift parameter," which accounts for differing choices of cost function (calculation of the difference between the predicted and true values that is used during model fitting). The reproduction is then converted back to linear space.

Thus, the UMs each have two free parameters which are fitted over all stimuli in each condition using least-square fits with the Matlab function *lsqnonlin*. For details concerning mathematics and justification for model structure, please refer to Petzschner & Glasauer's 2011 publication (Petzschner & Glasauer, 2011).

Bimodal Model: Integrated Likelihood Model

The Bayesian two-stage model used for the UMs was adapted to explain bimodal integration of vestibular and visual information. The measurement noise values, r_{vis} and r_{vest}, reflect the variance of the likelihood distribution for each modality. Because process noise was assumed to be equal across conditions and assigned a fixed value of 1, we will refer to the fitted r/q parameter as simply "r" in the following equation. When the unimodal likelihood distributions are combined into a bimodal likelihood, we can calculate the measurement noise associated with the bimodal likelihood as follows:

$$r_{bi} = \sigma_{bi}^2 \triangleq \frac{1}{\frac{1}{\sigma_{vis}^2} + \frac{1}{\sigma_{vest}^2}} = \frac{1}{\frac{{\sigma_{vest}}^2}{{\sigma_{vis}}^2{\sigma_{vest}}^2} + \frac{{\sigma_{vis}}^2}{{\sigma_{vis}}^2{\sigma_{vest}}^2}} = \frac{{\sigma_{vis}}^2{\sigma_{vest}}^2}{{\sigma_{vis}}^2 + {\sigma_{vest}}^2} = \frac{r_{vis}r_{vest}}{r_{vis} + r_{vest}} \quad (1)$$

The above equation is well established in its use to combine variances between two normal distributions and its behavior has also been previously documented (Figure 3) (Alais & Burr, 2004). Besides the computation of r_{bi}, the remainder of the ILM is identical to the UM. The reduction in measurement noise ultimately leads inlaid plots). It is important to note that the reduction in measurement, as compared to either unimodal measurement noise estimate, is proportional to the similarity of the respective UM noise estimates. Maximum benefit would be seen when r_{vest} equals r_{vis}.

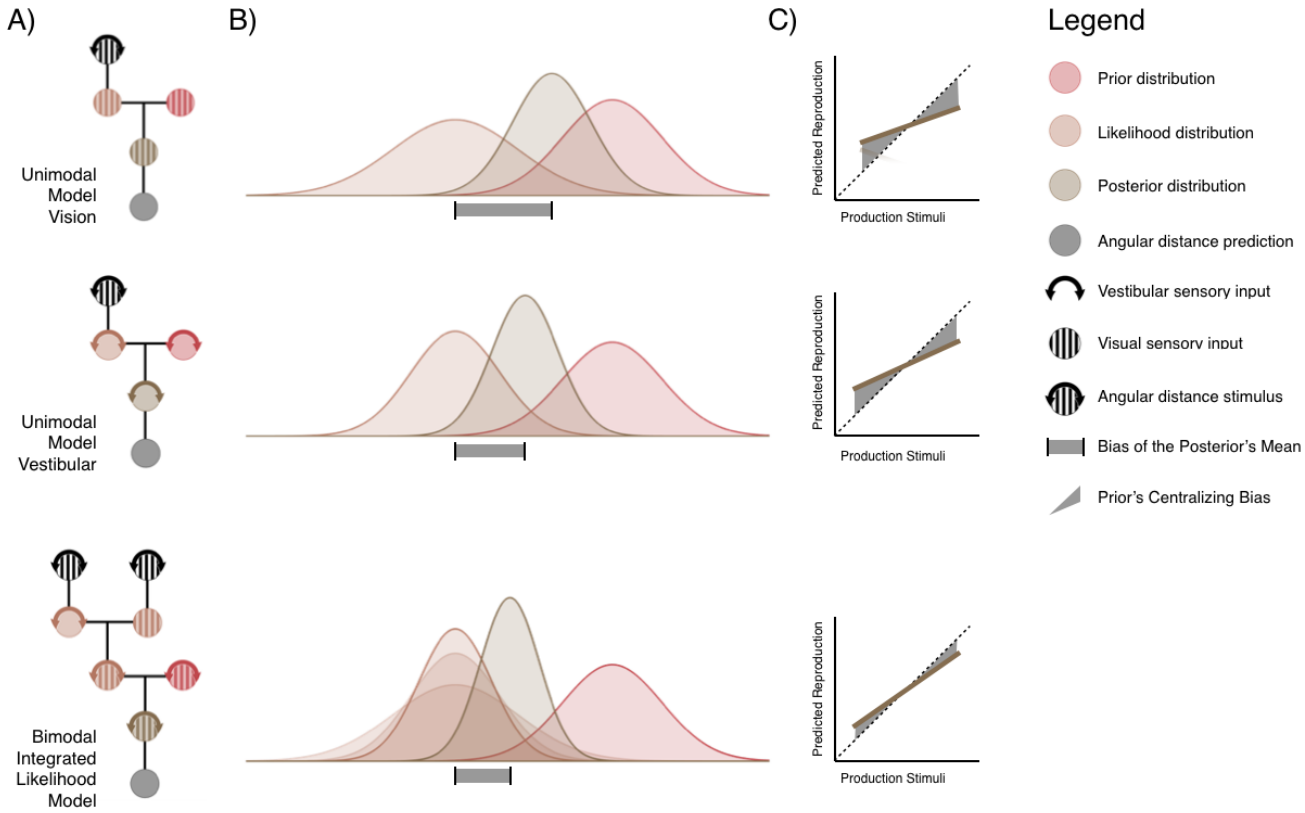

Figure 2. Illustration of model structures and source of the Prior's Centralizing Bias. (A) Each colored circle represents the probability density function with a Gaussian Distribution seen in B. The uncolored circles (the production stimuli and angular distance predictions) are discrete values. The Unimodal Models (UMs) are identical to the 2011 Petzschner and Glasauer two-stage model and either visual or vestibular input can be used. The Integrated Likelihood Model (ILM) contains modifications to account for multiple sensory inputs. Prior updating is not depicted here. Combinations of probability distributions, represented by horizontal connections between circles, constitute multiplication and result in an intermediate mean value, as well as a reduction in variance. **(B)** The differential width of likelihood distributions result in varied biases of the Posterior's mean from the Likelihood's mean (grey bars). For demonstrative purposes, all priors are portrayed to have the same mean and variance, although in practice both will vary based on incoming distance stimuli. The mean of the posterior distribution would be biased less toward the prior in the ILM than the UMs because the variance of the multisensory likelihood is the least. **(C)** A lesser bias toward the prior leads to angular distance predictions that are closer to the stimuli, which produces a smaller Prior's Centralizing Bias (PCB). In these illustrated plots of production stimuli versus predicted reproduction, we see that the ILM predictions have a heavily reduced PCB shown by an increase in the slope of the regression line.

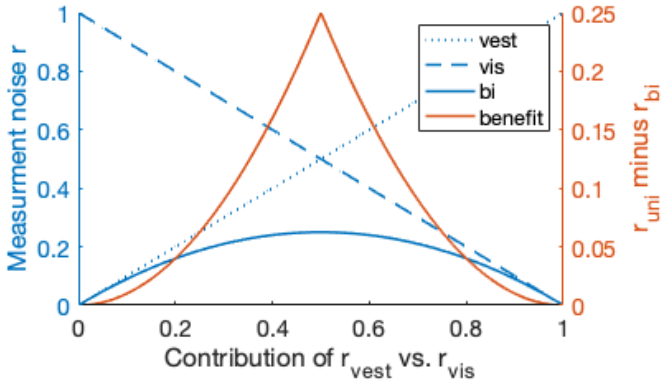

Figure 3: Benefit to bimodal measurement noise is dependent on the similarity of unimodal measurement noise. The figure is intended to show the non-linear reduction in bimodal noise as it relates to the relative size of unimodal measurement noises. The blue lines show theoretical values of measurement noise for the visual, vestibular, and bimodal conditions, where bimodal measurement noise is calculated according to equation 1. The red line shows the subtraction of the bimodal measurement noise values from the unimodal measurement noise values along the range of 0 to 1 and reflect the benefit of sensory fusion (reduction in measurement noise). The peak benefit occurs when unimodal values are equal.

Fitting Procedure

The UM was fit separately to the vestibular condition and the visual condition using least-squares fitting to attain estimates of the unimodal r/q ratios. The r/q ratios were then combined according to equation 1 to obtain a bimodal r/q ratio. When predicting data from the bimodal condition, all three models (ILM, visual UM, vestibular UM) had fixed r/q ratios taken/calculated from the unimodal conditions, but the shift parameters (see *Unimodal Models* point 4) were fitted anew. Shift parameters are refitted because the under-/over- estimation of angles between conditions is not constant though it was expected to be, according to the assumptions of the models. The relative fit of final predictions compared to participant reproductions in the bimodal condition was then examined.

Predicted PCB versus Actual PCB

To assure that the model predictions were exhibiting the same pattern of errors as the behavioral data, we calculated the PCB for each model's predictions and assessed the correlation with behavioral PCBs, expecting significant and positive Pearson's correlation coefficients. We also did the same for the bimodal condition data and the ILM predictions.

Goodness-of-fit

First, we calculated the coefficient of determination (R^2) for the UM model fit to the vestibular conditions and the visual condition. This value reflects the amount of variance in the behavioral reproductions, which can be explained by each unimodal model.

Next, we calculated the R^2 for each model's predictions of the bimodal condition data (Vestibular UM, Visual UM, and ILM), then compared the R^2 coefficients between models via a set of two-tailed paired t-tests. We were able to use the R^2, as opposed to a method that corrects for the number of free parameters like the Akaike Information Criterion, because all models have only one free parameter, the shift parameter, when predicting the bimodal data

RESULTS

Bimodal behavioral performance benefit

The 2-way repeated measures ANOVA of absolute behavioral error with factors 'experimental condition' and 'stimulus size' showed a significant main effect of stimulus size (F(4,255)=23.19,

p<0.001) and condition (F(2,255)=5.00, p=0.007), but no interaction effect. Similarly, the same ANOVA, performed for the standard deviation of errors, also found main effect of stimulus size (F(4,255)=14.53, p<0.001) and condition (F(2,255)=3.92, p=0.021), but no interaction. When comparing the visual unimodal condition and the bimodal condition via one-tailed paired t-tests, we found better performance in the bimodal condition in terms of accuracy (t(17)=1.94, p=0.034) and precision (t(17)=2.97, p=0.004). When comparing the vestibular unimodal condition and the bimodal condition via one-tailed paired t-tests, we also found better performance in the bimodal condition in terms of accuracy (t(17)=2.68, p=0.008) and precision (t(17)=2.28, p=0.018).

To examine the variability of accuracy within and across conditions, we plotted mean absolute behavioral error for all subjects and conditions. Behavioral error refers to the participants' responses minus the true values. The data was sorted based on the minimum signed difference between the unimodal condition's mean error and bimodal condition's mean error. Based on this visualization, 9 of 18 participants have mean errors in the bimodal condition that are clearly less than in both unimodal conditions (Figure 4C, right of line). For the other 9 participants, the mean errors in the bimodal condition are equal to or higher than in the unimodal conditions (Figure 4C, left of line).

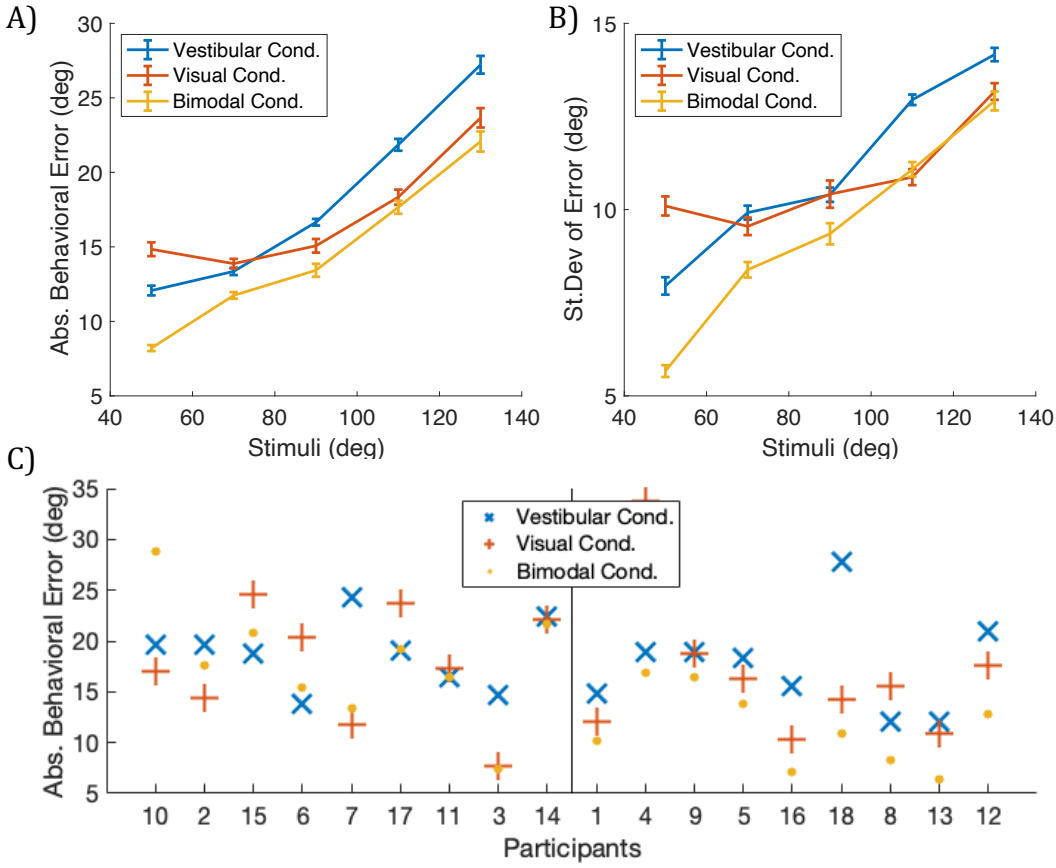

Figure 4. Performance benefit to accuracy and precision in the bimodal condition. A) Mean absolute behavioral error was computed for each condition and stimulus size combination and plotted here. The error bars are standard error. **B)** The mean variance of absolute errors was computed for each condition and stimulus size. The error bars are standard error. **C)** We plotted the mean absolute behavioral error for all subjects and conditions, and sorted the data based on the minimum signed difference between either unimodal condition error or bimodal condition error. The black line separates participants who showed a visually discernible decrease in error in the bimodal conditions when compared to both unimodal conditions.

Prior's Centralizing Bias (PCB)

The bimodal PCB was significantly lower than the vestibular unimodal PCB ($t(17)=2.46$, $p=0.012$) and the visual unimodal PCB ($t(17)=4.23$, $p<0.001$), demonstrating the same benefit to accuracy seen in the error analysis. From a Bayesian perspective, this also suggests that the prior for turn angle was relied upon less in the bimodal condition that in either unimodal condition.

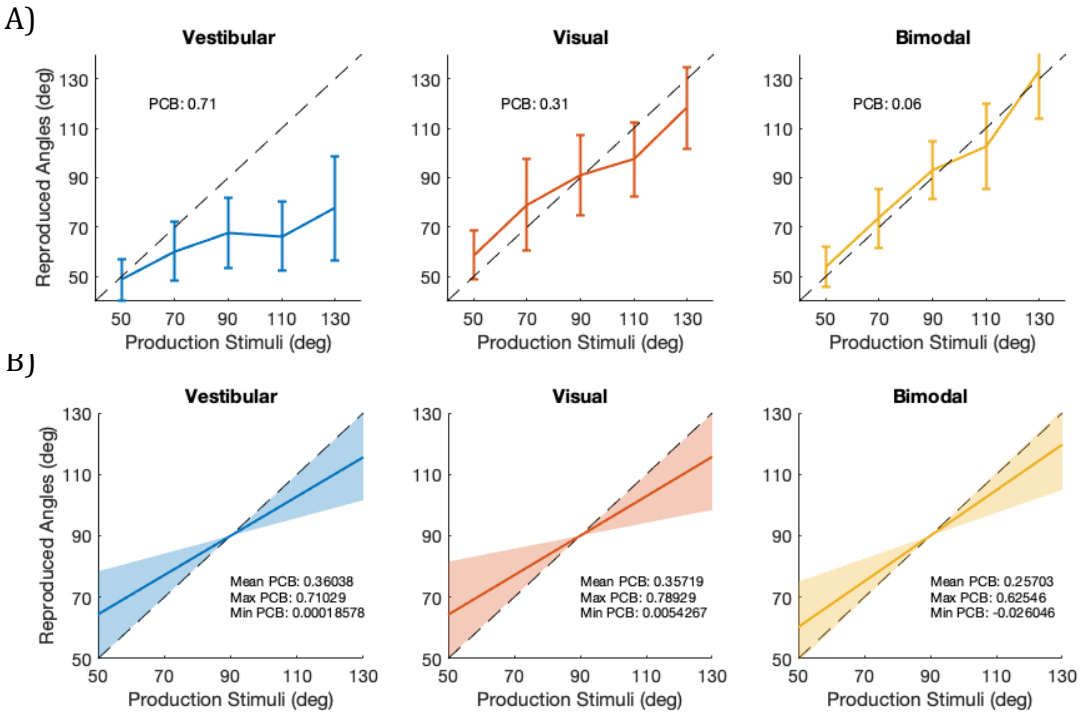

Figure 5. Comparison of the Prior's Centralizing Bias (PCB) between experimental conditions. A) Example of a single participant's performance in each condition. Not only are there differences in slope, but also a shift of the mean reproduction distance. **B)** The lines depicted here ignore the shift of the mean reproductions and only depict the slope of the fitted regression lines. The bold line in the middle shows the average slope of the reproduction-versus-production plot, and the shaded areas highlight the full range of slopes seen in each condition. The corresponding PCB-coefficients are overlaid on each plot.

Predicted PCB versus Actual PCB

The model predictions were plotted against the production stimuli in the same way as in 5A, and the PCB was calculated from the slope of the regression line. We found that predicted PCB for the unimodal conditions is significantly and positively correlated with actual PCB in both the vestibular condition ($r(17)=0.97$, $p<<0.001$) and the visual condition ($r(17)=0.94$, $p<<0.001$). In both cases, the offset of the regression line was close to zero, indicating that predictions showed a centralizing bias that was not consistently too large or small. The slope of the regression line was smaller than 1, indicating a scaling factor less than 1, which means that predictions tended to underestimate the centralizing bias when it was comparatively large. When the ILM was used to predict the bimodal condition data using the measurement noise parameters calculated from the unimodal data, we found that the predicted PCBs

were also highly correlated with the actual PCBs (r(17)=0.91, p<<0.001). The offset was close to zero and the scaling factor was around 0.75, which overall suggests that the PCB could be reliably predicted.

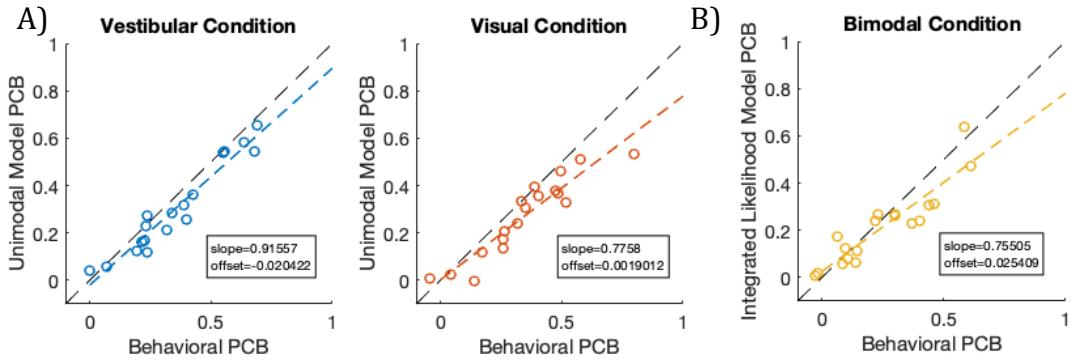

Figure 6: A) Correlations of the Prior's Centralizing Bias (PCB) coefficients for the unimodal model predictions and behavioral data from the unimodal conditions. In both cases we found a significant and positive correlation. The vertical offset indicates a global under- or over-prediction, and the scaling factor (slope) shows if accuracy of predictions changes across the range of PCBs in the data. **B)** Correlation of the bimodal behavioral PCB with the PCB predicted by the ILM was positive and significant. An offset close to zero and a scaling factor near 1, suggest accurate predictions of the PCB in the bimodal condition based on the unimodal noise parameters.

Unimodal model fit to the unimodal conditions

By calculating the coefficient of determination (R^2), we found that the Vestibular UM explained 53.4% of the variance in the vestibular condition data, with a standard deviation of 22.4%. Similarly, the Visual UM explained 51.1% of the variance in the visual condition data with a standard deviation of 28.4% (for individual results, see Supplementary Table 1).

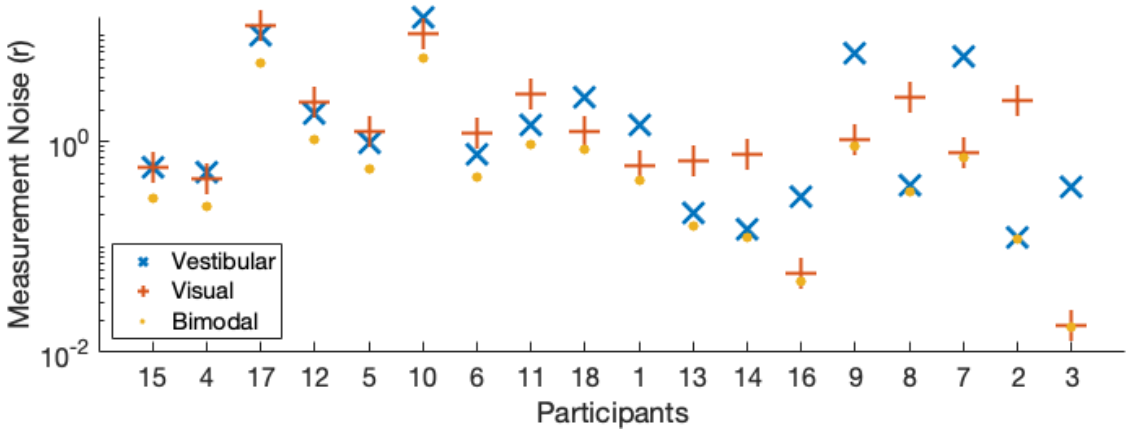

Figure 7: Unimodal measurement noise derived from UM fits and calculated bimodal measurement noise. On the x-axis, participants were sorted based on the absolute difference between the unimodal measurement noise values, with large differences on the right. There is a wide range of differences between the unimodal measurement noise parameters and, for individual participants, neither sensory modality has consistently lower or higher measurement noise than the other. The measurement noise values are plotted on a logarithmic scale because the Bayesian integration in our Bayesian models occur in log-space (see Methods) and it enables easier comparison of measurement noise values.

Predictions of the bimodal condition

Mean R^2 was calculated for model predictions of the bimodal condition for each subject and all models, and then compared with two-tailed paired sample t-tests. We found a small but significant advantage of the ILM when fitting the bimodal data as compared to the Vestibular UM (t(17)=2.65, p=0.017) and the Visual UM (t(17)=2.60, p=0.019). From the individual participant's R^2 coefficients, which are plotted behind the bars in figure 8A, we can see that often a UM fits the data similarly to the ILM, hence the small effect size (see Supplementary Table 1 for R^2 coefficients). To further inform the discussion concerning why we see such a small effect size, we performed two post-hoc correlations. In each correlation, we first calculated the difference between unimodal measurement noise (r_{vis} or r_{vest}) and bimodal measurement noise (r_{bi}; calculated according to equation 1). We correlated these differences with the difference in R^2 between the corresponding UM and the ILM. We found a significant negative correlation between the change in measurement noise and the differential goodness-of-fit for the vestibular data (r(17)=-0.80, p<0.001), and of the visual data (r(17)=-0.52, p=0.027). This indicates that the ILM fits the bimodal condition data better than the UMs, when we see a larger reduction in measurement noise. Conversely, when the unimodal and bimodal measurement noise is similar, the UM fits similarly to the ILM.

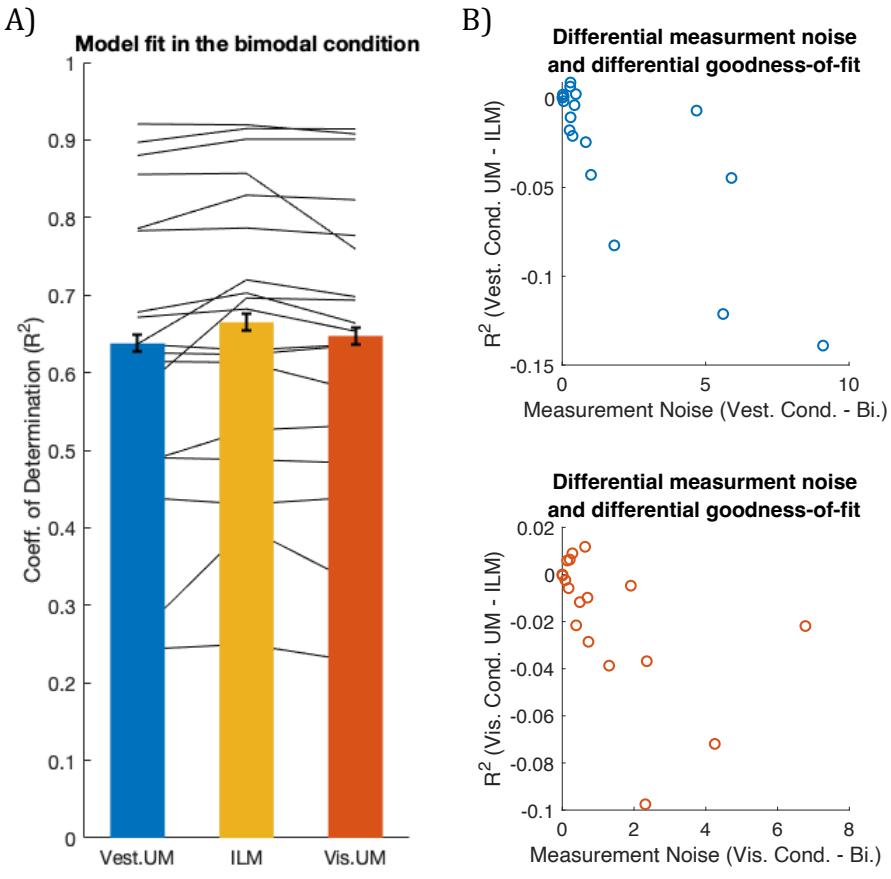

Figure 8: A) Comparison of unimodal model fits and the ILM fit of the bimodal condition data. We see a small but significant advantage of the ILM over the visual UM and the vestibular UM. Error bars are the standard error and the lines in the background show R^2 values for the individual participants (see Supplementary Table 1 for the values themselves) **B) Post-hoc correlations between change in measurement noise and the differential goodness-of-fit.** On the x-axis of each plot is difference between unimodal measurement noise and the calculated bimodal measurement noise. On the y-axis is the difference between the R^2s of UM predictions and ILM predictions. We see a significant negative correlation in the vestibular and visual plots, indicating that the ILM fits the bimodal condition data better than the UMs, when we see a larger reduction in measurement noise. Conversely, when the unimodal and bimodal measurement noise is similar, the UM fits similarly to the ILM.

DISCUSSION

Our expectations were that due to the process of sensory fusion, all participants should have improved accuracy and precision in the bimodal condition when compared to both the visual and vestibular unimodal conditions. Furthermore, we expected the Prior's Centralizing Bias (PCB) to decrease, which reflects not only improved accuracy but potentially a decreased reliance on a Bayesian prior (Jazayeri & Shadlen, 2010; Petzschner & Glasauer, 2011; Roach et al., 2017). Our behavioral results validate all these expectations, thereby suggesting that on average our pool of participants did fuse the visual and vestibular sensory information.

Our secondary goal was to see if we could accurately predict responses in the unimodal condition using our Bayesian models. Overall fit as assessed by the coefficient of determination (R^2) was moderate, explaining around 50% of the variance in behavioral reproductions. However, the average trends and systematic errors (PCB) were accurately predicted, as demonstrated by the close agreement between predicted and actual PCBs. Interestingly we see smaller R^2 coefficients in the UM fit of the unimodal conditions than in the UM fits to the bimodal condition. It may therefore be the case that the inherent noisiness of measurements in the unimodal conditions led to additional random errors that the Bayesian model could not account for. Given the relative variability of behavioral errors (Figure 4B) when compared to the production stimuli and the mean behavioral errors (Figure 4A), the authors consider the fit of the UMs to be sufficiently high.

The next investigation was to see if we could predict the responses in the bimodal condition based on the reproduction data from the unimodal conditions. Results showed that calculating the bimodal measurement noise, based on estimates of unimodal measurement noise, allowed the ILM to explain more than 60% of the variance in participant reproduction data. Furthermore, the predicted PCBs were closely matched to actual PCBs in the bimodal condition, showing that the ILM accurately predicted the degree to which accuracy increased. Matching the PCBs also confirms the established relationship between likelihood variance (analogous to measurement noise in our case) and weighting of the prior. Namely, as the variance of the likelihood diminishes, the influence of the likelihood on the posterior distribution increases, and consequently the influence of the prior decreases. It appears that we can accurately predict the influence of the prior on participant's reproductions (as reflected by PCB) by calculating the decrease in likelihood variance according to Bayesian sensory fusion (equation 1).

Lastly, we wanted to see if the ILM predicted the bimodal condition data better than the UMs. This was an important step because the relative weighting of the prior was more important than the influence of a prior in general. Although we did see that the ILM fit the bimodal condition data significantly better than both UMs, the effect size is notably small. The cause is clearly that for many participants one of the UMs can explain the bimodal data about as well as the ILM. At first alarming, this small effect size is actually expected (Alais & Burr, 2004) and relates directly to how the ratio of unimodal likelihood variances (r_{vis} and r_{vest}) impact the calculated variance of the multimodal likelihood (r_{bi}, Figure 3). This mathematical relationship is clearly outlined by Alais & Burr (2004) who apply maximum likelihood estimation (MLE) when fitting their models in the context of multi-sensory integration. Like us, they see the largest predicted benefits in situations where the unimodal likelihood distributions have similar variances. In situations with different unimodal variances, bimodal predictions lay closer to the unimodal predictions for the modality with lower variance. For us, an example would be if the estimated measurement noise from the visual condition is much lower than the estimated measurement noise from the vestibular condition (see participant 3, Figure 7). In this

case, the calculated bimodal measurement noise would be very similar to the visual measurement noise, and consequently the ILM predictions would also then be similar to the visual UM predictions. This is why we see the correlations in Figure 8B. In cases where the bimodal measurement noise is much smaller than the unimodal measurement noise, we see a clear difference between the ILM and UM fit. Previous research has provided experimental evidence for the dynamic inherent to equation 1 by manipulating the reliability (variance) of one sense in order to impact performance in the bimodal condition (Battaglia et al., 2003; Kaliuzhna et al., 2015; Prsa et al., 2012). Here we have provided additional evidence by showing that the same principal applies to pre-existing individual differences in inter-sensory measurement noise.

Given that the sensory modality with lower measurement noise contributes more to the calculation of bimodal measurement noise, one could say a participant might favor the more reliable (less noisy) modality over the other. A preference for one sensory modality over another is very well documented in multi-sensory integration literature (Battaglia et al., 2003; Knill & Saunders, 2003), including experiments with visual and vestibular interactions (Butler et al., 2010; Fetsch et al., 2009; Prsa et al., 2012). Rather than a consistent preference towards one modality, we see an equal occurrence of preference for the visual or vestibular modalities (Figure 7). One explanation for why a participant could have favored the vestibular modality is that visual information could be underweighted due to uncertainty regarding its origin, i.e. if it is caused by self-motion or motion in the environment (Fetsch et al., 2009). This is possible, since in the visual condition the environment was moving instead of the participant. Many participants reported that sometimes they were unsure if they were moving or if the drum was. If this were true, this would be a limitation of our experimental design since we cannot account for this influence in the bimodal condition. Still, this would only apply to participants who had higher visual measurement noise than vestibular measurement noise. Thus, it seems the most likely explanation is still that inter-sensory preferences express naturally in people and vary among individuals.

Participants who may not have fused

A closer look at behavioral errors in individual participants shows that the majority have reduced error in their behavioral condition, but some other participants have either less error in one of their unimodal conditions or less error in both unimodal conditions (Figure 4C, left side). These participants may have failed to successfully fuse the visual and vestibular sensory inputs because we do not see a benefit to performance. However, it is unlikely that this reveals a general inability of these participants to fuse visual and vestibular input. Probably it is due to the unnatural experimental separation of the visual and vestibular modalities. Recent research has proposed that not only are the visual and vestibular inputs normally fused, fusion is in fact mandatory (Prsa et al., 2012). In other words, even under circumstances where fusion of visual and vestibular information is unproductive, it occurs nonetheless. It has been found that the more correlated two senses are, the more likely they are to be fused. A wonderful example of this dictum is that participants can be taught to fuse two completely unrelated sensory inputs like luminance and haptic stiffness (Ernst, 2007) or vision and vestibular self-motion around different axis (Kaliuzhna et al., 2015). Given that visual and vestibular inputs measuring yaw-rotation are exceptionally consistent under normal circumstances, even if fusion were not mandatory, it would be deeply entrenched.

Conclusion

The visual and vestibular unimodal models fit their respective conditions suitably well and predict the PCB seen in the behavioral reproductions, indicating that participants are using prior information. Our Integrated Likelihood Model was able to accurately predict behavioral reproductions in the bimodal condition by combining unimodal measurement noise according to optimal fusion of unimodal variances. Not only that, but the ILM outperformed both UMs in the bimodal condition, strongly suggesting that our participants were fusing visual and vestibular sensory inputs in a Bayesian manner based on the variance of the likelihood distributions associated with each sensory modality.

REFERENCES

Alais, D., & Burr, D. (2004). The Ventriloquist Effect Results from Near-Optimal Bimodal Integration. *Current Biology*, *14*(3), 257–262. https://doi.org/10.1016/j.cub.2004.01.029

Battaglia, P. W., Jacobs, R. A., & Aslin, R. N. (2003). Bayesian integration of visual and auditory signals for spatial localization. *Journal of the Optical Society of America. A, Optics, Image Science, and Vision*, *20*(7), 1391–1397.

Butler, J. S., Smith, S. T., Campos, J. L., & Bulthoff, H. H. (2010). Bayesian integration of visual and vestibular signals for heading. *Journal of Vision*, *10*(11), 23–23. https://doi.org/10.1167/10.11.23

Dehaene, S., Izard, V., Spelke, E., & Pica, P. (2008). Log or Linear? Distinct Intuitions of the Number Scale in Western and Amazonian Indigene Cultures. *Science*, *320*(5880), 1217–1220. https://doi.org/10.1126/science.1156540

Durgin, F. H., Akagi, M., Gallistel, C. R., & Haiken, W. (2009). The precision of locomotor odometry in humans. *Experimental Brain Research*, *193*(3), 429–436. https://doi.org/10.1007/s00221-008-1640-1

Ernst, M. O. (2007). Learning to integrate arbitrary signals from vision and touch. *Journal of Vision*, *7*(5), 7. https://doi.org/10.1167/7.5.7

Ernst, M. O., & Banks, M. S. (2002). Humans integrate visual and haptic information in a statistically optimal fashion. *Nature*, *415*(6870), 429–433. https://doi.org/10.1038/415429a

Ernst, M. O., & Bülthoff, H. H. (2004). Merging the senses into a robust percept. *Trends in Cognitive Sciences*, *8*(4), 162–169. https://doi.org/10.1016/j.tics.2004.02.002

Fetsch, C. R., Turner, A. H., DeAngelis, G. C., & Angelaki, D. E. (2009). Dynamic Reweighting of Visual and Vestibular Cues during Self-Motion Perception. *Journal of Neuroscience*, *29*(49), 15601–15612. https://doi.org/10.1523/JNEUROSCI.2574-09.2009

Hillis, J. M., Watt, S. J., Landy, M. S., & Banks, M. S. (2004). Slant from texture and disparity cues: Optimal cue combination. *Journal of Vision*, *4*(12), 1. https://doi.org/10.1167/4.12.1

Hollingworth, H. L. (1910). The central tendency of judgment. *The Journal of Philosophy, Psychology and Scientific Methods*, *7*(17), 461–469.

Jacobs, R. A. (1999). Optimal integration of texture and motion cues to depth. *Vision Research*, *39*(21), 3621–3629.

Jazayeri, M., & Shadlen, M. N. (2010). Temporal context calibrates interval timing. *Nature Neuroscience*, *13*(8), 1020–1026. https://doi.org/10.1038/nn.2590

Jürgens, R., & Becker, W. (2006). Perception of angular displacement without landmarks: Evidence for Bayesian fusion of vestibular, optokinetic, podokinesthetic, and cognitive information. *Experimental Brain Research*, *174*(3), 528–543. https://doi.org/10.1007/s00221-006-0486-7

Kaliuzhna, M., Prsa, M., Gale, S., Lee, S. J., & Blanke, O. (2015). Learning to integrate contradictory multisensory self-motion cue pairings. *Journal of Vision*, *15*(1), 10–10. https://doi.org/10.1167/15.1.10

Kalman, R. E. (1960). A New Approach to Linear Filtering and Prediction Problems. *Journal of Basic Engineering*, *82*(1), 35–45. https://doi.org/10.1115/1.3662552

Kayser, C., & Shams, L. (2015). Multisensory Causal Inference in the Brain. *PLOS Biology*, *13*(2), e1002075. https://doi.org/10.1371/journal.pbio.1002075

Knill, D. C., & Saunders, J. A. (2003). Do humans optimally integrate stereo and texture information for judgments of surface slant? *Vision Research*, *43*(24), 2539–2558. https://doi.org/10.1016/S0042-6989(03)00458-9

Körding, K. P., Beierholm, U., Ma, W. J., Quartz, S., Tenenbaum, J. B., & Shams, L. (2007). Causal Inference in Multisensory Perception. *PLoS ONE*, *2*(9), e943. https://doi.org/10.1371/journal.pone.0000943

Landy, M. S., Maloney, L. T., Johnston, E. B., & Young, M. (1995). Measurement and modeling of depth cue combination: In defense of weak fusion. *Vision Research*, *35*(3), 389–412.

Loomis, J. M., Klatzky, R. L., Golledge, R. G., Cicinelli, J. G., Pellegrino, J. W., & Fry, P. A. (1993). Nonvisual navigation by blind and sighted: Assessment of path integration ability. *Journal of Experimental Psychology: General*, *122*(1), 73–91. https://doi.org/10.1037/0096-3445.122.1.73

May, M., & Klatzky, R. L. (2000). Path integration while ignoring irrelevant movement. *Journal of Experimental Psychology: Learning, Memory, and Cognition*, *26*(1), 169–186. https://doi.org/10.1037/0278-7393.26.1.169

Olkkonen, M., McCarthy, P. F., & Allred, S. R. (2014). The central tendency bias in color perception: Effects of internal and external noise. *Journal of Vision*, *14*(11), 5–5. https://doi.org/10.1167/14.11.5

Petzschner, F. H., & Glasauer, S. (2011). Iterative Bayesian Estimation as an Explanation for Range and Regression Effects: A Study on Human Path Integration. *Journal of Neuroscience*, *31*(47), 17220–17229. https://doi.org/10.1523/JNEUROSCI.2028-11.2011

Petzschner, F. H., Glasauer, S., & Stephan, K. E. (2015). A Bayesian perspective on magnitude estimation. *Trends in Cognitive Sciences*, *19*(5), 285–293. https://doi.org/10.1016/j.tics.2015.03.002

Prsa, M., Gale, S., & Blanke, O. (2012). Self-motion leads to mandatory cue fusion across sensory modalities. *Journal of Neurophysiology*, *108*(8), 2282–2291. https://doi.org/10.1152/jn.00439.2012

Roach, N. W., McGraw, P. V., Whitaker, D. J., & Heron, J. (2017). Generalization of prior information for rapid Bayesian time estimation. *Proceedings of the National Academy of Sciences*, *114*(2), 412–417. https://doi.org/10.1073/pnas.1610706114

Stocker, A. A., & Simoncelli, E. P. (2006). Noise characteristics and prior expectations in human visual speed perception. *Nature Neuroscience*, *9*(4), 578–585. https://doi.org/10.1038/nn1669

van Beers, R. J., Sittig, A. C., & Gon, J. J. (1999). Integration of proprioceptive and visual position-information: An experimentally supported model. *Journal of Neurophysiology*, *81*(3), 1355–1364. https://doi.org/10.1152/jn.1999.81.3.1355

van Beers, R. J., Wolpert, D. M., & Haggard, P. (2002). When feeling is more important than seeing in sensorimotor adaptation. *Current Biology: CB*, *12*(10), 834–837.

van Dam, L. C. J., Parise, C. V., & Ernst, M. O. (2014). Modeling Multisensory Integration. In D. J. Bennett & C. S. Hill (Eds.), *Sensory Integration and the Unity of Consciousness* (pp. 209–229). The MIT Press. https://doi.org/10.7551/mitpress/9780262027786.003.0010

SUPPLEMENTARY MATERIALS

		UNIMODAL CONDITION FITS		BIMODAL CONDITION FITS		
		Vestibular UM	Visual UM	Vestibular UM	Visual UM	ILM
		R2	R2	R2	R2	R2
PARTICPANTS	1	0.60	0.66	0.79	0.82	0.83
	2	0.60	0.52	0.61	0.58	0.61
	3	0.74	0.91	0.88	0.90	0.90
	4	0.67	0.72	0.64	0.64	0.63
	5	0.71	0.52	0.78	0.78	0.79
	6	0.68	0.44	0.67	0.65	0.68
	7	0.21	0.65	0.57	0.69	0.70
	8	0.73	0.52	0.86	0.76	0.86
	9	0.32	0.26	0.48	0.53	0.53
	10	0.08	0.22	0.26	0.33	0.40
	11	0.49	0.47	0.49	0.48	0.49
	12	0.62	0.61	0.68	0.66	0.70
	13	0.77	0.79	0.92	0.91	0.92
	14	0.74	0.50	0.63	0.64	0.62
	15	0.43	0.37	0.44	0.44	0.43
	16	0.71	0.82	0.90	0.91	0.91
	17	0.37	-0.36	0.24	0.23	0.25
	18	0.14	0.58	0.64	0.70	0.72
AVERAGE		**0.53**	**0.51**	**0.64**	**0.65**	**0.66**
STANDARD DEVIATION		**0.22**	**0.28**	**0.20**	**0.19**	**0.19**

Supplementary Table 1. Goodness-of-fit measures for individual participants. The coefficient of determination (R^2) is provided for all model fits and indicates the amount of variance explained by each model.

CHAPTER 3: Navigational Strategies

Triangle completion experiments

The practice of blind-folding participants and asking them to walk along the perimeter of a triangle is truly time-honored and has taken many variations over the years. Some examples included: having participants memorize the triangle and walk around it repeatedly by themselves (Glasauer et al., 2002), guiding the participant through part of the triangle and asking them to retrace their steps (Loomis et al., 1993), or guiding them through part of the triangle and having them complete the missing pieces by themselves. In one case, participants were guided along the hypotenuse and asked to walk the other two sides of a right triangle (Worchel, 1951). However, the most common variant is that participants are guided along 2 legs of a triangle and asked to complete the third side (Fujita et al., 1993; Harootonian et al., 2020; Klatzky et al., 1990, 1999; Loomis et al., 1993; Wiener et al., 2010).

This last version of the triangle completion task is analogous to foraging behavior demonstrated by many animals, since the goal is to end up at the start location (the beginning of the first leg of the triangle). The animal will make trips away from their nest or home location in order to find food, and then return back via a straight path (Heinze et al., 2018). These foraging journeys are often convoluted explorations, sometimes over great distances. For example, the Egyptian fruit bats will fly tens of kilometers away from their cave, but are still able to navigate back via a more-of-less straight route (Tsoar et al., 2011). In order perform the blindfolded triangle completion task, it is necessary to compute a “homing vector” which represents the distance and angle from the current location back to the home location.

Bayesian priors are maintained for estimated values during continuous and configural navigation strategies

Joshua W.G. Yudice[1], Stefan Glasauer[1]

1. Brandenburg University of Technology Cottbus-Senftenberg, Platz der Deutschen Einheit 1, 03046 Cottbus, Germany

ABSTRACT

Recent research by Wiener et. al. (2010) on path integration in humans demonstrated that when people are given specific instructions concerning a navigation strategy, they can flexibly switch between two dissociable strategy types: the configural strategy and the continuous strategy. They also showed that users of the continuous strategy tend to deviate their head's direction towards the goal location. In this experiment, 23 participants completed a similar triangle completion task but were not instructed to use a specific strategy. By retrospectively classifying participants into strategy type based on head deviation and confirming a similar pattern of results seen by Wiener et. al., we provide additional evidence to their hypothesis. We also show, through a combination of the behavioral results and the application of 2 Bayesian models, that in the absence of specific instructions participants may not naturally employ each strategy in its purest form. Many participants appear to use elements from both strategies, and all seem to maintain Bayesian priors for the return distance and angle composing a homing vector. However, only participants who use the configural strategy maintain Bayesian priors for the first 2 legs of the triangle and the turn angle between them, which were traversed before returning to the starting location. In summary, modeling the influence of Bayesian priors on navigation behavior offers a more nuanced understanding of employed navigation strategies in the absence of explicit instructions.

INTRODUCTION

Idiothetic Path Integration (iPI) is a process that allows an agent to track their position in space using only self-motion information, such as information from the vestibular and proprioceptive senses (Mittelstaedt & Mittelstaedt, 2001). Although it has been shown to be vulnerable to noise accumulation, there is compelling evidence to suggest that path integration provides a framework for constructing more complex representations of space (Biegler, 2000; Cheung & Vickerstaff, 2010; Schatz et al., 1999). In research on animals, where foraging journeys are often focal, it has been generally assumed that the studied animal uses a homing strategy, where it constantly updates a homing vector that points from its current position back towards the starting location (Heinze et al., 2018; Shettleworth, 2010). Whereas research on human participants has historically assumed that people perform path integration in an offline step after the outgoing path was completed (Fujita et al., 1993; Loomis et al., 1993). This latter approach requires that people monitor the distances and angles while walking, but integrate them only directly before the return journey. In their 2010 publication, Wiener et al. named the former strategy the "continuous strategy," in which the navigator constantly updates their homing vector, and the latter strategy the "configural strategy", in which the configuration of the outgoing paths are remembered. Fundamentally, they asked why the strategy typically associated with animals was not also considered for humans, and then demonstrated that humans can also continuously update a homing vector. By providing different instructions to their participants, the same participant could navigate using either the "continuous strategy" or the "configural strategy." In the absence of specific instructions, the authors speculate that an individual is likely to choose the strategy that is most appropriate to the task at hand (Wiener et al., 2010).

One way that Wiener et. al. differentiated the continuous and configural strategies was to measure performance on a so-called triangle completion task. During such a task, people are blindfolded and lead along 2 legs of a triangle before being asked to walk back to the starting location by themselves (return distance is C in Figure 1.2). Wiener et. al. measured performance with 4 metrics: Homing Error, Distance Error, Direction Error, and Response Time. The last metric is the time it took a participant to

decide upon and begin walking along the 3rd leg of the triangle. In the continuous strategy, integration of changes in distance and angle occur constantly, which means that the navigator always knows their position, but error associated with updating position and orientation also accumulate quickly (Cheung & Vickerstaff, 2010). Summarily said: response time is low, but overall error is high. In the configural strategy, response time is higher because the entire computation of the homing vector occurs just before executing the return path (Fujita et al., 1993). Error tends to be lower though, partially because updating occurs less often, but also because participants tend to use step counting to reduce uncertainty in distance estimates.

Perhaps the more important differentiating factor presented in Wiener et. al.'s 2010 paper, is that head direction predicts which strategy the participant is using. They found that during the triangle's second leg, participants' head direction significantly deviated from straight ahead toward the starting location. Furthermore, this was much more pronounced during the continuous strategy than during the configural strategy. They hypothesize that this is a motor expression of top-down influences associated with the applied navigation strategy. Practically speaking, this provides us with a clear method of classifying participants as either continuous solvers or configural solvers.

The first goal of this manuscript is to apply the above findings to a pre-existing dataset from one of our triangle completion experiments. Unlike in Wiener et. al. 2010 paper, we intentionally provided instructions that did not bias the participant toward one strategy or the other. We can therefore retroactively classify participants into each navigation strategy based on their head direction's deviation and see if their performance metrics (error and response time) corroborate the classification. The experiment presented here has two conditions, one in which scalene triangles are provided to the participants and one in which only right triangles are provided to the participants. On average, the triangles in this experiment are smaller than those used by Weiner et. al. and consequently we expect to see ameliorated differences in homing error and direction error between strategies. This is expected because the continuous strategy will not accumulate sufficient error to differentiate it. We do however expect to see differences between strategies for response time and distance error because they are not as dependent on path length.

Persistent geometric features represented as Bayesian priors

In the 1990 publication from Fujita et al., the authors describe their model of path integration as "history free," meaning that "the navigator maintains no record of the actual pathway by which [they] arrived at a point (Fujita et al., 1990)." Indeed many of the numerous investigations into path integration via mathematical modeling are also history-free (see (Vickerstaff & Cheung, 2010) for review), but we know from literature on magnitude estimation that prior experience has a substantial influence on current estimates of magnitudes (Petzschner et al., 2015). Obviously, estimating distances and angles is crucial to the process of path integration, and thus it is essential that we consider how prior experience may be influencing navigation behavior during the continuous and configural strategies.

In the triangle completion experiments, all employed navigation strategies must ultimately produce the homing vector, but the configural and continuous strategies differ in terms of which geometric features need to be remembered. In the configural strategy, the distances of the first 2 triangle legs and the intervening angle must be remembered until they are ultimately integrated at the end of the second triangle leg (A, B, and ϕ in Figure 1.2). But in the continuous strategy we assume that the

homing vector is updated after each triangle and turn, instead of at the end. After walking the first leg of the triangle and before beginning to walk the second leg of the triangle, (after A and before B in Figure 1.2) the participant would be remembering the updated homing vector and not the completed distance and angle anymore. In a Bayesian context, in which prior experience is maintained as a probabilistic distribution called a prior distribution (or simply a "prior"), we might expect priors to exist for the remembered information in each strategy. We hypothesize that these priors would cause very specific biases in the corresponding geometric features, leading to different response patterns between strategies.

To investigate the role of prior information in these navigation strategies, we will build upon a Bayesian model proposed by Petzschner & Glasauer in 2011 that iteratively updates the mean of its prior based on each incoming stimulus. This model is preferable over others because it explains a variety of well-known behavioral effects, but it is exceptionally efficient in its use of free parameters (Glasauer, 2019; Petzschner & Glasauer, 2011). We include multiple instances of this model in each of our models (Figures 2). Our model that corresponds more with the configural strategy is called the Trigonometric Model (TM) because it maintains priors for the leg and angle components of a triangle (Figure 1, A, B, and ϕ). In this model, the homing vector is calculated *after* the priors will bias the estimates for the first two legs of the triangle and the intervening angle. Our second model is named the Egocentric Model (EM), because it maintains priors for egocentric turn angle and return distance (Figure 1, C and θ). It also only computes the homing vector at the end of the triangle, which is not representative of the continuous strategy, but our hypothesis concerns the information maintained between trials and not the online performance during trials. What is important in the EM, is that the homing vector is calculated *before* Bayesian Integration, and thus the priors bias the return distance and angle.

This brings us to the second goal of this manuscript, which is to investigate if there exists a differential use of prior information between the navigation strategies proposed by Wiener et. al. We would expect the EM predictions to fit the data of continuous solvers better than TM predictions. Similarly, we would expect the TM predictions to fit the data of configural solvers better than EM predictions. We hope to reveal this by looking at the success of each model in their predictions based on explained variance and the overall size of errors between predicted and true values.

If the author's expectations are fulfilled, we will provide a demonstration of the hypothesis set forth by Wiener et. al. in 2010: namely that head deviation toward the goal can predict navigation strategy. We would also establish a modeling framework that could be used to confirm which navigation strategy was used by each participant and predict their trial-by-trial responses. Lastly, we would provide evidence that prior information is not only being used for, but predictably biases, navigation.

METHODS

Participants

Data was collected for 23 participants (10 female) with a mean age of 29.8 years old (SD=5.3 years). Participants were informed about the general experimental procedure and their rights regarding personal data before the experiment began. Upon completion they were paid 10 euro per hour for their participation.

Materials

Due to the demolition of the initial testing space, the experiments took place in two separate rooms. The first 13 participants were collected in room with dimension of approximately 6.7 x 5.7 meters and the latter 10 participants were collected in a much larger room with a free testing space greater than 10 meters x 7 meters. The first room contained 8 infrared motion tracking cameras (Qualisys) mounted

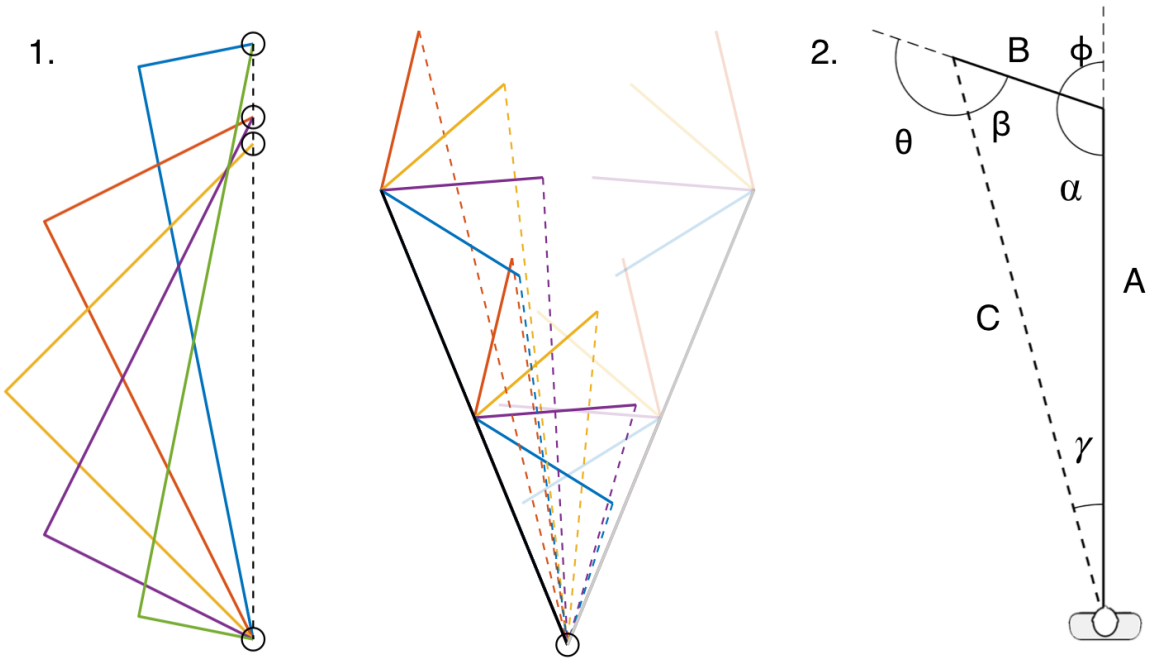

Figure 1: 1. Triangular paths used in the Right Triangle Condition (RTC, left) and the Scalene Triangle Condition (STC, right). RTC: There are 4 starting locations. indicated by black circles. Each path was traversed in both directions, so that: both the first and second legs of a triangle could take all 5 possible distance values and both turn directions could be included. All ideal return paths followed the black dotted line and the first turn was always 90 degrees. **STC:** All triangles shared the same starting location, indicated by the black circle. The first leg of triangles could be either 1.6 meters or 3.2 meters, and the second leg was always 1.2 meters. The angle of the first turn could take 1 of 4 values: 36, 72, 108, or 144 degrees. The faded paths on the right side perfectly mirror the opaque paths on the left, and in these triangles the first turn was towards the left. **2. Reference notation for triangle legs and angles.** The two turns, ϕ and θ, are calculated as 180 degrees minus α and 180 degrees minus β, respectively. In the triangle completion experiment, the participant is guided blindfolded from position AC along leg A to position AB, is turned there by ϕ degrees, then guided along leg B to corner BC. At BC, the participant is asked to turn and walk home to the starting position. A correct response would thus require turning θ degree to the left, then walk the distance C and stop at the starting location.

	SCALENE TRIANGLE CONDITION	RIGHT TRIANGLE CONDITION
LEG A	1.6, 3.2	0.7, 1.4, 2.1, 2.8, 3.5
LEG B	1.2	0.7, 1.4, 2.1, 2.8, 3.5
LEG C	0.95, 1.68, 2.28, 2.34, 2.67, 3.05, 3.75, 4.23	2.97, 3.13, 3.57
ALPHA	36, 72, 108, 144	90
BETA	20.66, 26.40, 41.93, 54.27, 65.12, 86.03, 95.73, 126.44	11.30, 26.57, 45, 63.43, 78.69
GAMMA	9.60, 15.34, 17.55, 17.72, 21.97, 30.07, 42.88, 48.27	11.30, 26.57, 45, 63.43, 78.69

Table 1: Dimensions of triangle paths in each condition. All unique values are listed for each condition and measure. Lengths are in meters and angles are in degrees

overhead, whereas the second contained 1 additional camera to accommodate the larger space. Sufficient tracking accuracy was possible in both spaces. Participants wore a helmet fitted with 5 infrared reflecting balls (2 cm diameter), each mounted on a 12 cm pole, such that at least 3 balls were visible from every angle. Participants were both blindfolded and given headphones, over which white noise was played so that audio and visual cues were denied. Triangles of varying dimensions were taped onto the floor of the room and marked with identification codes. Data from the cameras was recorded using the Qualisys software installed on a desktop PC. The experimenter recorded relevant time points using key presses on a wireless keyboard.

We administered two experimental conditions, each of which was designed to manipulate the theoretical outcomes of the models: the Scalene Triangle Condition (STC) and the Right Triangle Condition (RTC) (Figure 1.1). In the STC, the first leg of each triangle could take two lengths, either 1.6 meters or 3.2 meters, while the second leg was always 1.2 meters. The angle between legs was either 36, 72, 108, or 144 degrees and both left and right turns were possible. Each unique triangle was completed twice, resulting in a total number of 32 trials. The starting location in the room was always the same (Figure 2A). In the Right Triangle Condition (RTC), all triangles were right triangles where the first and second legs could take any of the following lengths: 0.7, 1.4, 2.1, 2.8, or 3.5 meters. Left and right turns were both possible and each unique triangle was repeated 3 times, resulting in a total of 30 trials. Unlike the STC, where starting location was always the same, the RTC had 4 possible starting locations.

Experimental Procedure

Participants were greeted in a different area than the experiment room and informed about the experiment's structure and about policies concerning data usage before they consented to participate. Afterwards the experimenter demonstrated the task, confirmed understanding, and then the participant was prepared for participation before being led to the experiment room. Before beginning each condition, the participant was led through practice trials until they demonstrated an understanding of the task. During these instructions the experimenter was very careful not to bias the participants towards a navigational strategy beyond the unavoidable influence of the task demands themselves.

In each trial, the participant was gently led by their shoulders along the first leg of the triangle, turned once, and led along the second leg. Once at the end, their task was to first turn so that they faced the starting location and then walk in a straight line until they reached that location. After the participant had verbally confirmed their decision, the experimenter lead the participant on a circuitous and random walk through the room to disorient them between trials.

Each condition lasted around 45 minutes and the order that conditions were provided was counterbalanced among participants. Trial order was random but fixed across participants. After each condition, the participant was asked four questions concerning sensory input, insight into the experiment, and navigation strategy (Supplementary Table 1).

Data Acquisition

Raw position and orientation data from the Qualisys software was interpolated and smoothed before turn angle and leg length were automatically identified in Matlab using custom scripts. Data was visually inspected for quality and 19 trials (across all Participants) were excluded due to missing data.

Categorizing Strategy from Head Deviation

Head deviation during leg B of the triangle was calculated as follows: 1) calculate the participant's straight trajectory from triangle corner AB to corner BC 2) subtract the participant's head direction (yaw-axis) at every time-point from the straight-ahead 3) modify the sign of the result, such that positive was towards the *perceived* goal (i.e. deviated to the left when corner AB was a left turn). We then looked at the distribution of average head direction in triangle leg B across all trials. Participants whose head deviation was significantly greater than 0, as assessed at a 95% confidence interval, were considered to use the continuous strategy. All other participants were assumed to have used the configural strategy.

Behavioral Metrics

To reflect the analysis done by Wiener et al. 2010, we implemented the same 4 behavioral metrics: distance error, direction error, homing error, and response time.

1) Distance error: The participant's reproduction of triangle leg C (distance from their actual position at corner BC to their final estimate of the start location) minus the true value of leg C (distance from their actual position at corner BC to their starting location on that trial). Negative values indicate an underestimation of the true distance.
2) Direction error: The participant's reproduction of angle θ (how far they turned before walking) minus the true return angle (that would have oriented them directly towards their starting position on that trial). Positive values indicate an overestimation of return angle.
3) Homing error: The distance between their starting location on that trial minus their final estimate of the starting location. Distances are always positive.
4) Response Time: The amount of time between when they stopped at corner BC until they exited an imaginary circle around the stop location with a radius of 40 cm. Response Time therefore includes their decision time, time taken to turn towards the perceived starting location, and time taken to walk 40 cm.

In the original publication, a 2x2 repeated measures ANOVA was done for each metric using path length and navigation strategy as factors. Then t-tests were conducted to compare navigation strategies within the long and short path lengths. We imitate this by also conducting an ANOVA for each metric but with experimental condition and navigation strategy as factors, then we compare navigation strategy within each condition using t-tests. Given the differences between our experimental designs, all t-tests were conducted for completeness, although not all were expected to be significant. Although the original publican did not correct for multiple comparisons, we grouped the statistical tests by metric and corrected the significance threshold via the Holm-Bonferroni method

Linear statistics are applied for analyzing angular data here for two reasons: firstly, for reproducibility, and secondly because linear statistics are equally appropriate in our case. The primary concern when analyzing angle, was that there exists a clockwise and counterclockwise rotation that both point to the

starting location, but participants always turned the shorter of the two angles, so this ambiguity was removed. We also analyze only magnitudes and the differences between them, and magnitudes do not exhibit the cyclical and bounded characteristics of circular data. Sign was added after magnitudes were calculated to denote over or underestimations.

Model Design

Two computational models were formulated which include the two-stage generative Bayesian model postulated by Petzschner and Glasauer in 2011. The unchanged model is nested within each of our models multiple times (e.g. Figure 2, green highlighted area). The model is highly flexible, in that it can take any measure as input, iteratively produce predictions of that measure, and maintain a Bayesian prior for said measure. The following paragraphs will describe this model in more detail, however for specific mathematics and the reasoning underlying its structure, please refer to the original publication.

The 2-stage Bayesian model proposed by Petzschner and Glasauer iteratively predicts incoming stimuli on a trial-wise basis. In each iteration, the incoming stimulus is converted into log-space to attain the mean of the Bayesian likelihood distribution. This probability distribution is assumed to be Gaussian, as are all other distributions in log-space. This transformation into log-space is done to mirror the Weber–Fechner law, which has been applied to magnitude estimation in other contexts (Dehaene et al., 2008; Durgin et al., 2009; Jürgens & Becker, 2006; Stocker & Simoncelli, 2006). Also, as part of the transformation, the stimuli is divided by a small normalizing constant which has the same units as the stimuli itself. This makes the likelihood unitless and can be used to modulate the flatness of the log function. In all cases, we used the constant 0.01 as was done in the original publication.

Next, the means of the likelihood and prior distributions are combined to obtain the posterior probability distribution's mean using a weighted summation. Normally, the weights of the likelihood's mean and the prior's mean is determined by the relative variances of the two distributions. But in this case, the weights during summation are determined by a free parameter called the r/q ratio, which is the ratio of measurement noise (r, variance of the likelihood) to process noise (q, variance during prior update). In the first iteration of the model, the mean of the prior is initialized to the log-transformed stimulus value. Afterwards, the prior's mean is updated on every trial via a weighted sum of the current likelihood's mean and the mean of the prior from the previous iteration. The weights during this summation are determined by a 1-dimension derivation of the Kalman filter that relies on the r/q ratio.

The model's final prediction is the mode (maximum) of the posterior distribution plus a fitted constant (shift parameter), which accounts for the use of different cost functions. In summary, a single instance of this model has two free parameters: the r/q ratio and the shift parameter. Our implementation of the model has two important caveats regarding the shift parameter: firstly, we interpret it as an additive gain to predictions, not to explain cost functions. Secondly, for angles, we use 2 separate shift parameters for different turn directions, since there was a difference in additive bias in some Participants.

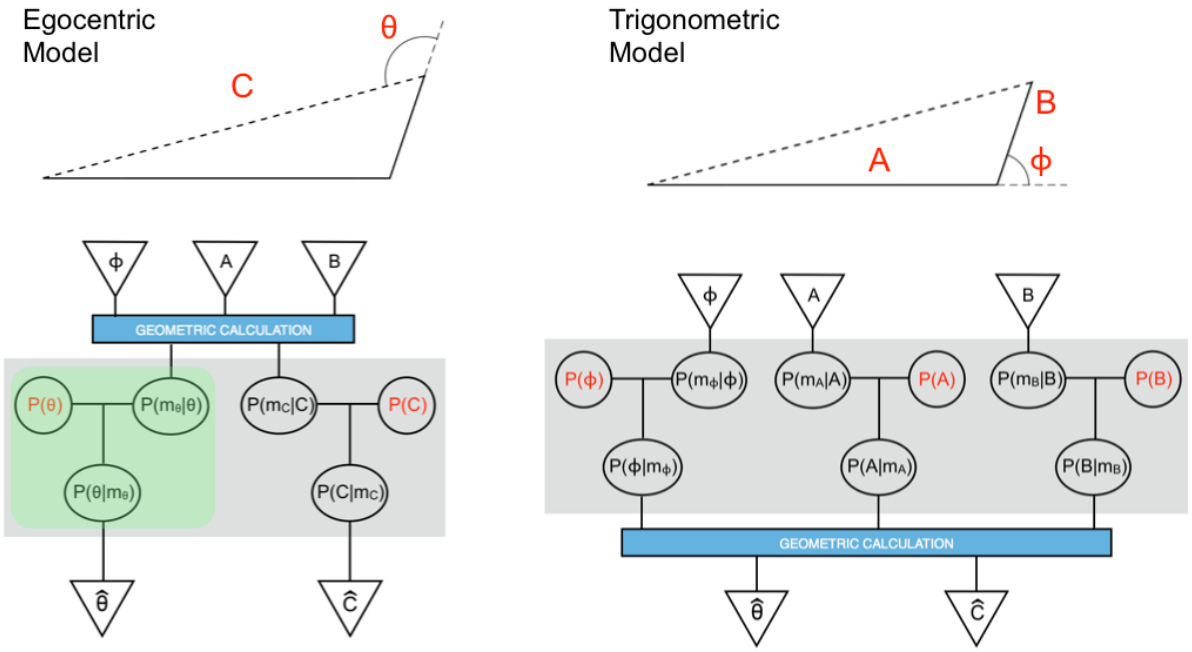

Figure 2: Differing structures of the 2 generative Bayesian models. The piece of the model highlighted in green represents the computational unit that is identical to the Petzschner and Glasauer 2011 two-stage model. This unit is repeated multiple times in each model depending on how many priors are maintained. The blue rectangles represent geometric calculations necessary to compute an angle or edge from available information. All models receive the first two legs (A, B) and the first turn angle (ϕ) as inputs. Furthermore, they all predict the second turn angle (θ) and return distance (C). **Left:** The Egocentric Model (EM) maintains a prior for the reproduced turn (θ) and reproduced distance (C). **Right:** The Trigonometric Model (TM) maintains three priors, one for each leg of the triangle (A, B) and the angle of the first turn (ϕ).

As seen in Figure 2, the 2-stage Bayesian model above occurs multiple times in each model: two times for the EM and three times for the TM.

Egocentric model: Return distance (leg C) and return angle (θ) are calculated from legs A and B, and angle ϕ, and afterwards used as inputs for the Bayesian integration. Two priors are maintained, one for the return distance and one for the return angle. There are 5 free parameters in total: 2 r/q ratios and 3 shift parameters for each metric (2 for angle).

Trigonometric model: Three priors are maintained, one for the distance of leg A, one for leg B, and one prior for the angle ϕ between these legs. Internally, the model predicts all three values and then geometrically calculates the return angle and distance. The TM was designed to also have 5 free parameters by using the same r/q parameter for both distances, A and B, and applying the shift parameters after the geometric calculations of return angle θ and return distance C. Since the influence of the prior on estimates is mediated only by the r/q ratio, this should not undermine a comparison between the models.

Fitting Procedure

The EM and TM were fitted to the STC data using non-linear least-squares fitting (MATLAB function *lsqnonlin*). To ensure consistency between the models and concurrent fitting of all metrics, the fitting procedure minimized the linear distance between predicted final position and the participants' actual final position over all trials. The fitted values for the r/q ratios from the STC were used to predict the

RTC data, but the shift parameters were not used. This was done primarily because the Petzschner & Glasauer model assumes that participants have a constant tendency toward over/under-estimation across conditions, and we expected this not to be true. Therefore, when predicting the RTC, the r/q ratios carried over from the STC and the shift parameters were fitted anew. The averages and standard deviation of the fitted parameters for each model can be found in Supplementary Table 3.

Comparing Predictions to Responses

We assessed how well the models' predictions fit the participant responses by calculating a positional coefficient of determination (pR^2, equation 1). The numerator of the fraction in equation 1, is the Residual Sum of Squares (RSS) for the linear distance between the predicted home location and the participant's estimated home location, which is in fact the term that was minimized during the non-linear least-squares fitting. The denominator is the Total Sum of Squares (TSS), which quantifies the variation in participant's estimates of starting location, i.e. their final location in each trial.

$$pR^2 = 1 - \frac{RSS}{TSS} = 1 - \frac{\sum_{i=1}^{n}(x_i - \hat{x}_i)^2 + (y_i - \hat{x}_i)^2}{\sum_{i=1}^{n}(x_i - \bar{x})^2 + (y_i - \bar{y})^2} \quad (1)$$

This is a convenient measure of goodness-of-fit since it considers both distance and angle.

We further compared model performance between the two navigation strategies (as classified by head deviation) by calculating the root-mean-square error (RMSE) for distance, angle, and final position (again predicted home location minus estimated home location). We can utilize the $pR^2$and RMSE instead of a method that corrects for the number of free parameters, like the Akaike Information Criterion, because both the EM and TM have 5 free parameters and thus, we do not expect that the TM will have an advantage. We corrected for multiple comparisons by grouping the statistical tests according to 4 constituent assertions necessary to show that the EM and TM fit their corresponding solving strategy. In each case, we used at least n of 4 related to the 4 metrics (pR^2 and 3 RMSE measures) and corrected via the Holm-Bonferroni method.

RESULTS

We first verified that participants had successfully performed the task by looking at: the correlation between individual participant responses and the stimulus values, as well as the median absolute error (absolute value of responses minus stimulus) (Supplementary Table 2). In most cases, correlation between the distance or angle stimuli and participant responses was high (R>0.5), indicating that participants were on task and generally successful. Median absolute error across both conditions were as follows: 22.9 degrees error for return angle θ, 0.55 meter error for return distance C, and 1.33 meter error for homing distance. One exception of note is that in the Right Triangle Condition (RTC), distance estimates did not vary in accordance with the stimuli. This indicates that these participants, especially those with low correlation and high error, were not able to differentiate between the different distance stimuli.

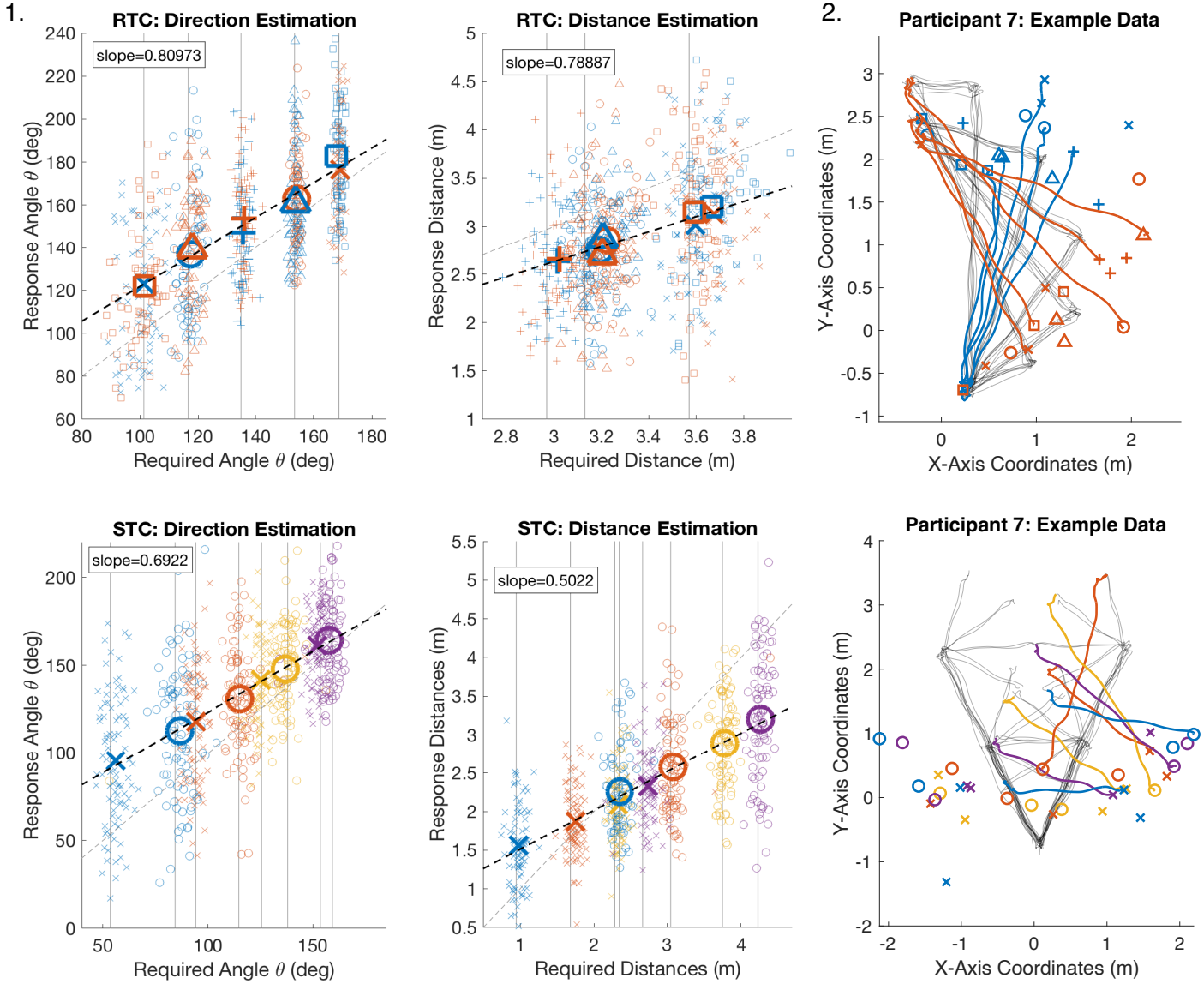

Figure 3.1. Average trends in response-vs.-required plots. Bottom row: The STC data from all participants was pooled and subdivided by outgoing path distance (shape) and turn angle α (color). Vertical grey lines show the ideal required values, the dashed grey line is the line of equality, and the regression line is dashed black. The slope of the regression line is shown in the white box for all plots. **Top row:** The RTC data from all participants was pooled and subdivided by turn direction (color) and triangle shape (shape). Otherwise, notation is the same as for the STC.

Figure 3.2. Exemplary triangles from participant 7. Plotted example paths have been interpolated, but not smoothed. **Top:** All final destinations in the RTC are plotted with the same shape and color combinations as in the response-vs.-required plots. Example paths are shown for each combination of turn direction and triangle geometry. **Bottom:** All final destinations in the STC are plotted with the same shape and color combinations as in the response-vs.-required plots. Example paths are shown for only one turn direction, but for each combination of outgoing

The Participants' reproductions of angle and distance were plotted against the stimuli to observe average trends (Figure 3). Data from all participants were pooled and averages were calculated for each triangle geometry. Of particular interest was if the slope of the regression line, which was fitted to the data, deviated from 1 as this can indicate a centralizing bias of reproductions by the prior distribution.

The computed averages of the behavioral estimations were well explained by a linear fit and the slopes of the regression lines were less than 1 for both distance and angle in both conditions. The slope could indicate a centralizing bias caused by the Bayesian priors (Jazayeri & Shadlen, 2010; Petzschner et al., 2015), where the strength of the prior's bias is proportional to 1 minus the slope (Petzschner & Glasauer, 2011). The vertical displacement of the regression lines in these plots show that angle was generally overestimated and distance was generally underestimated.

Differentiating Navigation Strategy

As part of the post-experiment interview, participants were asked if they used a strategy during the triangle completion task. Of the 23 participants, 5 reported not using a strategy, 3 indicated the use of an actively updated homing vector, 15 counted their steps, and 15 visualized the triangles geometry (Supplementary Table 1). Of the 3 that reported updating a homing vector, all said that they counted steps, and 1 said they also visualized the triangle geometry.

When looking at head-deviation from straight ahead during the second leg of the triangle, we found that 11 participants in the STC and 13 participants in the RTC had significant deviations towards the perceived starting location. We presumed that these participants were using the continuous strategy and that the other participants were using the configural strategy (Figure 4.1). Then we looked at group differences for each behavioral metric by performing a 2x2 repeated measures ANOVA with experimental condition and navigation strategy as factors (Figure 4.2).

Distance Error: We expected to see that distance error for configural solvers was closer to 0 than for continuous solvers. The 2x2 repeated measures ANOVA with experimental condition and navigation strategy as factors revealed a significant main effect of strategy ($F(1,22)=4.62$, $P=0.037$), but not condition. Nor was there an interaction. The differences between strategies were evaluated via 1-tailed t-tests assuming unequal variance and were found to be significant in the STC data ($t(1,20.8)=2.07$, $P=0.026$), but not in the RTC data $t(1,19.7)=1.16$, $P=0.129$).

Direction Error: Although Wiener et. al. showed lower direction error for the configural strategy, this was only true for long distance (average outgoing path length of 15.3 meters). Due the small size of our triangles in comparison to Wiener et. al., we did not expect to see differences in direction error. The 2x2 repeated measures ANOVA with experimental condition and navigation strategy as factors revealed no significant main effects or interaction. However, a t-test (1-tailed, unequal variance) showed that direction error in the RTC was indeed lower for the configural solvers ($t(1,20.8)=1.78$, $P=0.045$).

Response Time: We expected to see robust differences in response time between solving strategies because it does not rely on path length. However, the 2x2 repeated measures ANOVA with experimental condition and navigation strategy as factors revealed no significant main effects or

interaction. Furthermore, t-tests (1-tailed, unequal variance) for each condition were also not significant (RTC: t(1,16.6)=0.90, P=0.189, STC t(1,20.5)=0.32, P=0.374).

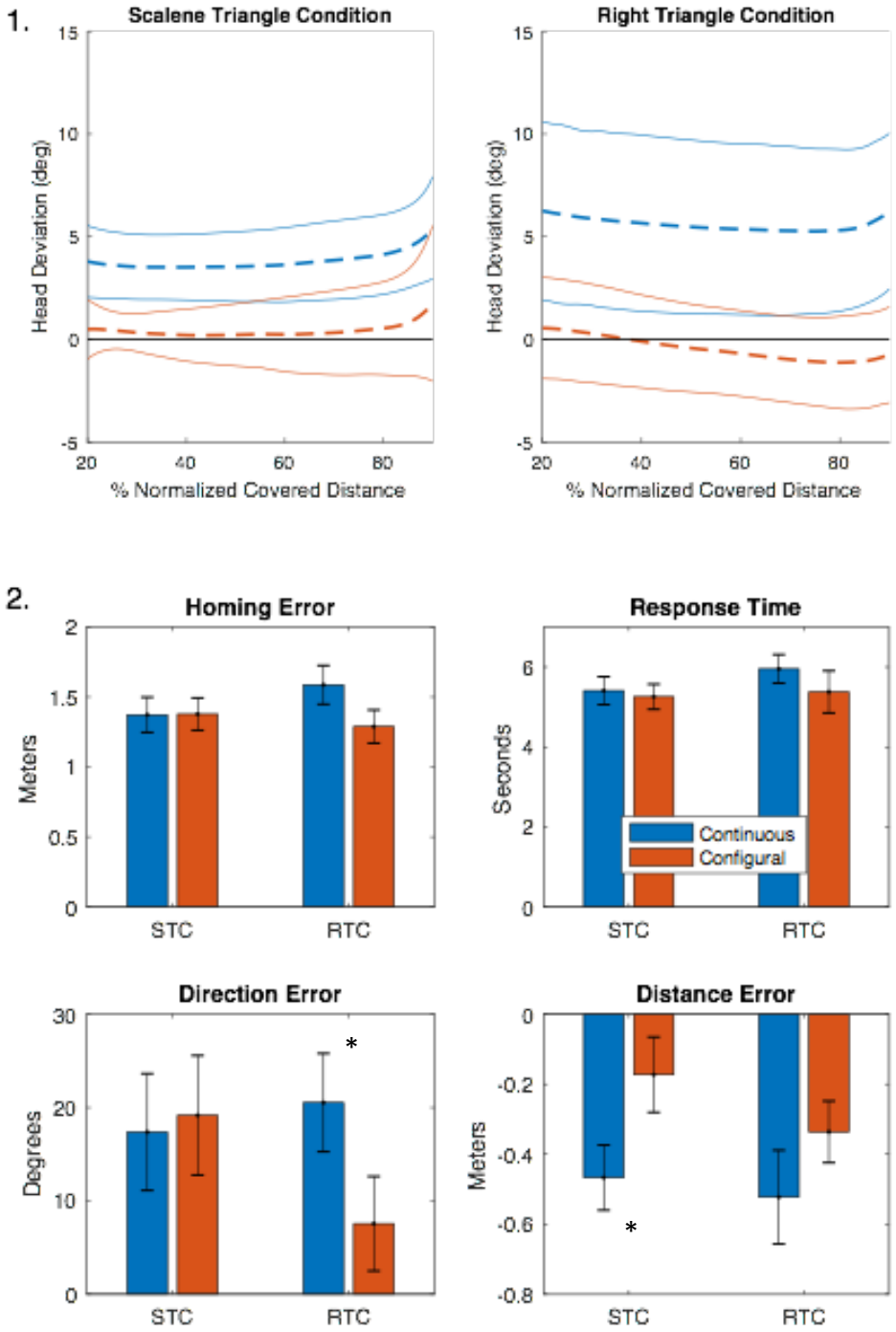

Figure 4: 1. Head deviation from straight ahead during leg B of each trial. The distance along leg B was normalized as the percentage of total length. Positive deviations are towards the goal location (subjective), and a participant was classified as a continuous-strategy user if their head deviation between 20% and 90% of the overall length was significantly greater than 0 (95% Confidence Interval). All other participants were considered to be configural strategy users. The dotted line indicates the mean and the solid lines are 1 standard error. **2. Response time and error metrics organized by navigation strategy and experimental condition.** Given the path lengths used in our experiment, we expected lower distance errors and higher response times for the configural-strategy users when compared to continuous-strategy users. This was only true for distance errors. We did however see unexpected differences between strategies for direction error data in the RTC, which conform with the hypothesis for Wiener et. al. 2010. Depicted error bars show the standard error.

Model Predictions

First the Egocentric Model (EM) and Trigonometric Model (TM) were fit to the STC data to obtain the free-parameter values. To ensure that these free-parameter values were meaningful, we evaluated their goodness-of-fit via a positional coefficient of determination (pR^2) and found that the EM and TM explained the behavioral data similarly well. On average, they both explained about 52% (±21%) of the variance in participant's final estimates of starting location.

We then applied the fitted ratios of measurement noise to system noise (*r/q*) from the STC data to predict the RTC data (see Methods: *Fitting Procedure*). Again, we calculated the pR^2 and found that the EM explained 45.5 ± 27.6% of the variance in participant's final estimates of starting location. The TM only explained 21.5 ± 30.3% of the variance, which was significantly less than the EM (paired t-test, t(1,22)=3.76, P=0.001).

We then divided up participants into navigation strategy users based on the head deviation and conducted a 2x2 repeated measures ANOVA with model type and navigation strategy as factors. The ANOVA revealed a main effect of model type (F(1,22)=9.46, P=0.006) and a main effect of navigation strategy (F(1,22)=8.45, P=0.004), but no significant interaction. We expected that the EM would explain the continuous strategy data better than the configural strategy data, and a 1-sided t-test with unequal variance revealed that this was not true (t(1,20.0)=1.55, P=0.93). In fact, the trend was reversed, though not significant as revealed by a post-hoc 2-sided t-test. Conversely, we expected that the TM would explain the configural strategy data better than the continuous strategy data, and another 1-sided t-test with unequal variance showed that this was very much true (t(1,20.7)=3.08, P=0.003). Although the effect was driven largely by an exceptionally poor fit of the TM to the continuous strategy data.

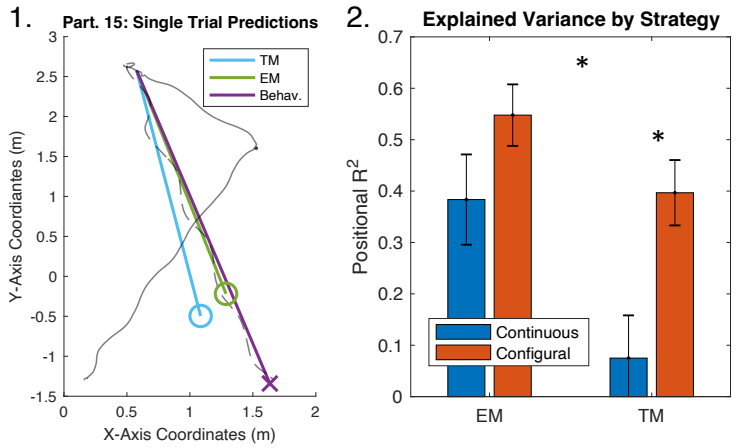

Figure 5: 1. Exemplary trial with model predictions. The distance between the circles and the x was minimized during model fitting and used to compute the numerator of the positional coefficient of determination. **2. Positional coefficient of determination, segregated by model type and navigational strategy.** Both the TM and EM fit the configural solvers' data better than the continuous solvers data. The EM explained more of the variance in final position estimates than the TM. Depicted error bars are standard error.

We further compared model fit over the RTC data by examining the root-mean-square error (RMSE) between model predictions and behavioral responses for direction, distance, and final position (Figure 6).

Direction RMSE: We conducted a 2x2 repeated measures ANOVA with model type and navigation strategy as factors and found a main effect of navigation strategy (F(1,22)=7.79, P=0.008) and model type (F(1,22)=5.8, P=0.021), but no interaction. The expectation that the TM would have lower RMSE for the configural solvers was evaluated via a 1-tailed t-test with unequal variance and found to be

significant (t(1,15.1)=2.13, P=0.025). However, the EM did not have lower RMSE for continuous solvers. A paired t-test revealed an overall lower RMSE for the EM (t(1,22)=3.98, P<0.001), indicating a generally better fit to the return angles.

Distance RMSE: The 2x2 repeated measures ANOVA with model type and navigation strategy as factors did not reveal any main effect nor interactions.

Final Position RMSE: The last 2x2 repeated measures ANOVA with model type and navigation strategy as factors revealed a main effect of model type (F(1,22)=6.18, P=0.017), but not navigation strategy and there also was not an interaction. A paired t-test revealed an overall lower RMSE for the EM (t(1,22)=3.91, P<0.001). This metric is complimentary to the pR^2, demonstrating additionally that the overall difference between the true final destinations and the predicted final destinations were less for the EM compared to the TM.

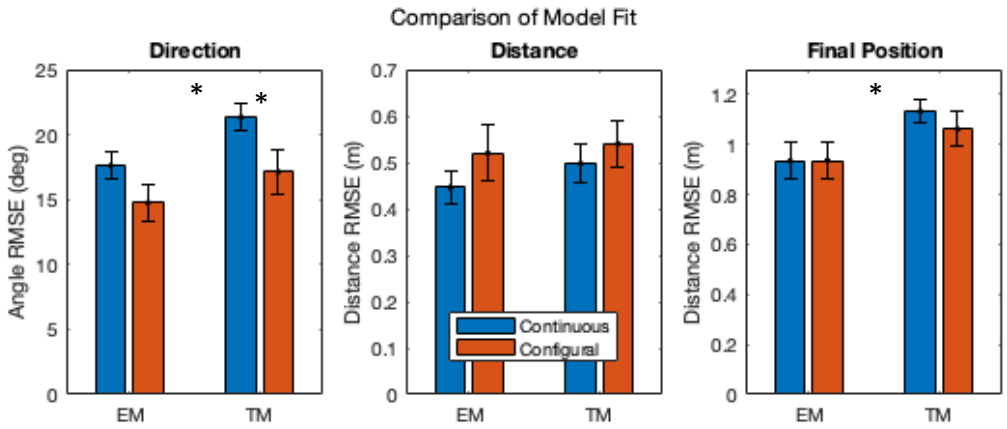

Figure 6: Bayesian models predict within-strategy responses similarly, but overall fit differs. The root-mean-squared error (RMSE) was calculated between the model predictions and behavioral responses. Not one of the two-factor ANOVAs conducted for each metric revealed a significant interaction between strategy and model, however, we did see a main effect of model for Direction RMSEs and Homing Distance RMSEs, which is due the fact that the EM's RMSE was lower than the TMs RMSE. We also found a main effect of navigation strategy for Direction RMSEs, confirming results from the positional coefficient of determination showing that both the EM and TM fit the configural solvers' data better. Depicted error bars are standard error.

DISCUSSION

At the outset of this investigation, we sought to fulfill 2 goals. First, we aimed to verify the results of Wiener et. al. 2010 by retrospectively classifying our participants based on head deviation. In the case that this classification was appropriate, we expected to see the same behavioral differences between solving strategies seen by Wiener et. al. The second goal of this manuscript was to determine if there exists a differential use of prior information between the navigation strategies proposed by Wiener et. al. We adopted a Bayesian model from the magnitude estimation literature (Petzschner & Glasauer, 2011), in order to construct 2 models that roughly correlated with the continuous and configural strategies in terms of which geometric quantities were the focus of each strategy. The Egocentric Model (EM) was expected to best fit data from the continuous solvers and the Trigonometric Model (TM) was expected to best fit data from the configural solvers.

Verifying the success of strategy classification

By lucky coincidence, we had a roughly equal distribution of navigation strategy users in both experimental conditions. When comparing strategies based on the behavioral metrics, some of the results were as we expected. We did not find a significant difference between strategies in homing error, which is presumably due to the much smaller dimensions of our triangles compared to those seen in Wiener et. al. We also found a significant difference between navigation strategies for distance error, which was not dependent on the size of the triangles in their data.

There were also some unexpected outcomes. Despite the small triangles in our experiment, when we analyzed direction error, there was a significant difference between navigation strategies in the RTC. The direction of errors was as we would have expected with larger triangles: smaller error for the configural solvers than for the continuous solvers. It could be the case that the RTC geometries (intermediate angle ϕ was always 90°) were much easier to integrate when using the configural strategy and thus this inter-strategy difference emerged. The higher slopes in the plots of behavioral response versus stimuli (Figure 3) would also suggest more accurate responses in the RTC when compared to the STC, suggesting that this condition was generally easier for our participants.

Thus far, evidence suggests that the classification of our participants by navigation strategy was successful, but there was one unexpected difference which refutes this conclusion: there was not a difference between response times. The response time was expected to be longer for the configural condition because at corner BC participants must take additional time to integrate the homing vector, whereas for continuous solvers the integration has been happening continuously. Furthermore, this effect should be present regardless of outgoing path length. The overall duration of response times was also unexpected. In Wiener et. al. 2010, the average response time for configural solvers was approximately 4 seconds and the average for continuous solvers was just less than 3 seconds. Our participants had average response times of approximately 5 seconds or more in all navigation strategies and experimental conditions.

One explanation could be that in the absence of specific instructions, our participants employed both navigation strategies to some extent. This hypothesis would be corroborated by the data from participant interviews, in which all participants who reported using a strategy also said they used some technique associated with the configural strategy: either step counting or visualizing the geometry of the triangle (Supplementary Table 1). Only three participants reported the additional use of a technique characteristic of the continuous strategy. That said, the head deviation data and the error metrics all suggest that some participants were using the continuous strategy. Thus, we would propose that head deviation does predict navigation strategy, but it may be the case that people do not employ either strategy alone, instead combining them to varying extents.

Modeling results

In essence, we used the Scalene Triangle Condition (STC) as a training data set for the free parameters of the models and used the Right Triangle Condition (RTC) as the test data set. The motivation for testing the data in the RTC, instead of the STC, is that to accurately estimate the noise-ratio parameter (measurement noise divided by system noise, see *Methods*) we need a range of stimuli. In the Trigonometric Model (RM), we have a noise-ratio that is associated with intermediate angle ϕ, but ϕ is

fixed to 90 degrees in the RTC. Therefore, the RTC data would not have been ideal for fitting the free parameters.

In general, the goodness-of-fit results were not as we expected but were interesting nevertheless. The TM did fit the configural solver's data better than the continuous solvers data, seemly because the TM fit the continuous solver's data especially poorly. However, the Egocentric Model (EM) also fit the configural solver's data better than the continuous solver's data. Overall and irrespective of navigation strategy, the EM explained more variance in the participants estimates of the goal location than the TM. What this suggests is that all participants were maintaining priors for return distance (leg C) and return angle (θ), at least to a greater extent than they maintained priors for distance of leg A, leg B, and the angle ϕ. Given how well the EM predictions matched the data from configural strategy users, it could be that priors for return distance and angle had an especially large influence on configural solver's responses.

One possibility is that the TM is unfounded and none of the participants were maintaining priors for leg A, leg B, and the angle ϕ. But this is refuted somewhat by the fact that the TM explained so little variance in the continuous solvers' data but did explain the configural solvers' data (Figure 5.2, right side). If the biasing influence of the priors on TM predictions did not somewhat mirror aspects of behavioral responses, then we would have expected consistently low pR^2 coefficients. Another more likely option would be that 1) the continuous solvers specifically did not maintain priors for leg A, leg B, and the angle ϕ, but the configural solvers did. And 2) both configural solvers and continuous solvers maintained priors for return distance and angle. In this case we would see that the EM fits both navigation strategies, but the TM only fits the configural strategy, which closely matches our modeling results.

The most likely conclusion is that we were wrong in assuming a 1:1 relationship between model type and navigation strategy. It may be the case that a prior is maintained for every metric that is estimated by the participant. In the configural strategy it is necessary to estimate leg A, leg B, and angle ϕ to later estimate return distance and return angle. In this case we might expect that a participant employs 5 priors, and this would certainly be an avenue of further testing. Whereas in the continuous strategy, the return distance and angle are the only metrics that are estimated and thus the EM would be appropriate in its use of 2 priors.

Combined outcome of behavioral and modeling results

The modeling results seem to conflict with our earlier hypothesis based on the behavioral analysis: that our participants were using both the continuous and configural strategies to varying extents. If the continuous solvers are not maintaining priors for leg A, leg B, and the angle ϕ, then that might mean that the continuous solvers are also not using the configural strategy. And if that is true, then we should have seen differences in response times in the behavioral data. So why were response times so long for the continuous solvers?

The problem might be with how we are defining the configural strategy. For example, although step counting is particularly helpful to the configural strategy, it does not mean a continuous solver couldn't count steps as well to improve estimations of traversed distance. It could be that continuous solvers are using a combination of techniques outside of a pure continuous strategy and this underlies the higher response times. There is some evidence to suggest that working memory load on a spatial task

can interact with counting performance (Shimomura & Kumada, 2011) and we know from the participant interviews that the majority of our participants were employing step counting. Unfortunately, we can only speculate as to the reason for these longer response times for continuous solvers, but this could be investigated in future experiments.

Explicit vs. implicit use of navigation strategy

One essential characteristic of path integration (PI) is that it happens automatically, regardless of the current task (May & Klatzky, 2000). In other words, our updating of position and orientation happens implicitly without explicit thought. In the Wiener et. al. paper, participant behavior is influenced by top-down modulation because participants are acting according to specific instructions. In our experiment, we did not provide such specific instructions, but most of our participants nevertheless chose to employ explicit strategies. Perhaps it is natural for humans to apply explicit strategy to a navigation task and therefore if we are assessing PI with a triangle completion task, we can expect our participants to count their steps, visualize the triangles' geometry as though drawn on paper, and use other techniques that they do not apply during everyday tasks where navigation is not the point of the task.

A potential limitation of this study is that that the use of priors by participants could be influenced by the explicit strategies that participants used. For example, maybe only participants who visualized the triangles' geometry maintained priors for legs 1 and 2 and the angle between them. We know that the use of the configural strategy is not inhibited by a concurrent task (May & Klatzky, 2000) and assuming that the continuous strategy isn't either, it would be interesting to perform this paper's analysis on participants who navigate while performing a concurrent task. This way, we would discourage the use of an explicit strategy and hopefully remove this confounding factor.

Conclusion

In this experiment, we provided additional evidence validating the hypothesis of Wiener et. al. that head deviation from straight ahead could be used to classify navigation strategy as continuous or configural. However, we also showed that participants may not naturally employ each strategy in its purest form, instead also adding techniques such as step counting to the continuous strategy. Lastly, we demonstrated that participants are likely employing a Bayesian prior in their execution of the Triangle Completion Task. It is also probable that users of both navigation strategies maintain a prior for return distance and angle, but only configural strategy users maintain priors for outgoing triangle legs and turn angles. The authors invite further research to determine if a Bayesian prior is used during navigation under more naturalistic conditions.

REFERENCES

Biegler, R. (2000). Possible uses of path integration in animal navigation. *Animal Learning & Behavior*, *28*(3), 257–277. https://doi.org/10.3758/BF03200260

Cheung, A., & Vickerstaff, R. (2010). Finding the Way with a Noisy Brain. *PLoS Computational Biology*, *6*(11), e1000992. https://doi.org/10.1371/journal.pcbi.1000992

Dehaene, S., Izard, V., Spelke, E., & Pica, P. (2008). Log or Linear? Distinct Intuitions of the Number Scale in Western and Amazonian Indigene Cultures. *Science*, *320*(5880), 1217–1220. https://doi.org/10.1126/science.1156540

Durgin, F. H., Akagi, M., Gallistel, C. R., & Haiken, W. (2009). The precision of locomotor odometry in humans. *Experimental Brain Research*, *193*(3), 429–436. https://doi.org/10.1007/s00221-008-1640-1

Fujita, N., Klatzky, R. L., Loomis, J. M., & Golledge, R. G. (1993). The Encoding-Error Model of Pathway Completion without Vision. *Geographical Analysis*, *25*(4), 295–314. https://doi.org/10.1111/j.1538-4632.1993.tb00300.x

Fujita, N., Loomis, J. M., Klatzky, R. L., & Golledge, R. G. (1990). A Minimal Representation for Dead-Reckoning Navigation: Updating the Homing Vector. *Geographical Analysis*, *22*(4), 324–335. https://doi.org/10.1111/j.1538-4632.1990.tb00214.x

Glasauer, S. (2019). Sequential Bayesian updating as a model for human perception. In *Progress in Brain Research* (Vol. 249, pp. 3–18). Elsevier. https://doi.org/10.1016/bs.pbr.2019.04.025

Heinze, S., Narendra, A., & Cheung, A. (2018). Principles of Insect Path Integration. *Current Biology*, *28*(17), 1043–1058. https://doi.org/10.1016/j.cub.2018.04.058

Jazayeri, M., & Shadlen, M. N. (2010). Temporal context calibrates interval timing. *Nature Neuroscience*, *13*(8), 1020–1026. https://doi.org/10.1038/nn.2590

Jürgens, R., & Becker, W. (2006). Perception of angular displacement without landmarks: Evidence for Bayesian fusion of vestibular, optokinetic, podokinesthetic, and cognitive information. *Experimental Brain Research*, *174*(3), 528–543. https://doi.org/10.1007/s00221-006-0486-7

Loomis, J. M., Klatzky, R. L., Golledge, R. G., Cicinelli, J. G., Pellegrino, J. W., & Fry, P. A. (1993). Nonvisual navigation by blind and sighted: Assessment of path integration ability. *Journal of Experimental Psychology: General*, *122*(1), 73–91. https://doi.org/10.1037/0096-3445.122.1.73

May, M., & Klatzky, R. L. (2000). Path integration while ignoring irrelevant movement. *Journal of Experimental Psychology: Learning, Memory, and Cognition*, *26*(1), 169–186. https://doi.org/10.1037/0278-7393.26.1.169

Mittelstaedt, M.-L., & Mittelstaedt, H. (2001). Idiothetic navigation in humans: Estimation of path length. *Experimental Brain Research*, *139*(3), 318–332. https://doi.org/10.1007/s002210100735

Petzschner, F. H., & Glasauer, S. (2011). Iterative Bayesian Estimation as an Explanation for Range and Regression Effects: A Study on Human Path Integration. *Journal of Neuroscience*, *31*(47), 17220–17229. https://doi.org/10.1523/JNEUROSCI.2028-11.2011

Petzschner, F. H., Glasauer, S., & Stephan, K. E. (2015). A Bayesian perspective on magnitude estimation. *Trends in Cognitive Sciences*, *19*(5), 285–293. https://doi.org/10.1016/j.tics.2015.03.002

Schatz, B., Chameron, S., Beugnon, G., & Collett, T. S. (1999). The use of path integration to guide route learning in ants. *Nature*, *399*(6738), 769–772. https://doi.org/10.1038/21625

Shettleworth, S. J. (2010). *Cognition, evolution, and behavior*. http://www.dawsonera.com/depp/reader/protected/external/AbstractView/S9780199717811

Shimomura, T., & Kumada, T. (2011). Spatial working memory load affects counting but not subitizing in enumeration. *Attention, Perception, & Psychophysics*, *73*(6), 1694–1709. https://doi.org/10.3758/s13414-011-0135-5

Stocker, A. A., & Simoncelli, E. P. (2006). Noise characteristics and prior expectations in human visual speed perception. *Nature Neuroscience*, *9*(4), 578–585. https://doi.org/10.1038/nn1669

Vickerstaff, R. J., & Cheung, A. (2010). Which coordinate system for modelling path integration? *Journal of Theoretical Biology*, *263*(2), 242–261. https://doi.org/10.1016/j.jtbi.2009.11.021

Wiener, J. M., Berthoz, A., & Wolbers, T. (2010). Dissociable cognitive mechanisms underlying human path integration. *Experimental Brain Research*, *208*(1), 61–71. https://doi.org/10.1007/s00221-010-2460-7

SUPPLEMENTARY MATERIALS

Post-experiment questions	
Q1	Could you hear any sounds besides my voice and the white noise?
Q2	Did you notice any specific differences between experimental sessions?
Q3	Did you notice a pattern with regards to the location of the home or turn positions?
Q4	Did you use a strategy to complete the experiment?

Part.	Q.1	Q.2	Q.3	Q.4	Notes
1	No	No	No	1	
2	No	No	No	0*	Imagined a tempo, but "beats" were not explicitly counted
3	No	No	No	2	
4	No	No	No	2	
5	No	No	No	1*, 2	Tried to regulate his step size. He pointed to the start at the end, but did not update a header while walking.
6	Yes*	No	No	2	Sometimes heard her own steps
7	Yes*	No*	No	1, 2	Thought the RTC triangles were longer
8	No	Yes*	No	0	Noticed the 90 degree angles in RTC, notices STC has more variable geometries
9	No	No	No	0	
10	No	Yes*	No	1, 3*	Noticed generally more obtuse Beta angles in STC as compared to RTC. His strategy involved imagining a ball at the start, which grew smaller as he walked away.
11	No	No	No	0	
12	No	No	Yes*	1, 2	Noticed the consistent start location in STC, but was nevertheless disoriented between trials
13	No	Yes*	No	1, 2	Noticed the 90 degree angles in RTC
14	No	No	No	1, 2	
15	No	No	No	0	
16	No	No	No	1, 2	
17	No	Yes*	No	1, 2	Noticed the 90 degree angles in RTC
18	No	No	No	1, 2	
19	No	No	No	1, 2, 3	
20	No	No	No	1, 3	
21	No	No	No	1, 2	
22	No	No	No	1, 2	
23	No	No	No	1, 2	

1 - Participants used some form of step counting.
2 - Participants visualized the triangles' dimensions to some degree.
3 - Participants used some kind of actively updated homing vector

Supplementary Table 1: Post-experiment questions and answers. After the completion of both experimental conditions, each participant was asked 4 questions in the order listed above. The questions were phrased such that participants should say "No" to all the above questions except the question concerning strategy, which was open-ended. Some participants did intuit qualities of the experimental design that could have improved their performance, and one participant could hear their own steps. However, these participants did not exhibit notably better performance on the task than others, so they were not excluded.

Part.	SCALENE TRIANGLE CONDITION							RIGHT TRIANGLE CONDITION						
	Angle (deg)			Distance (m)			Homing (m)	Angle (deg)			Distance (m)			Homing (m)
	Err	R	p	Err	R	p	Err	Err	R	p	Err	R	p	Err
1	26.70	0.60	0.001	0.95	0.69	0.000	1.70	12.28	0.80	0.000	0.99	0.31	0.096	1.32
2	12.22	0.90	0.000	0.35	0.93	0.000	0.81	11.02	0.82	0.000	0.89	0.31	0.100	1.10
3	13.57	0.90	0.000	0.70	0.77	0.000	0.97	10.60	0.86	0.000	0.75	0.18	0.350	1.11
4	21.56	0.67	0.000	0.43	0.77	0.000	1.18	11.40	0.76	0.000	0.30	0.60	0.000	0.83
5	14.92	0.86	0.000	0.56	0.55	0.002	0.96	16.44	0.74	0.000	0.56	0.50	0.005	1.07
6	49.44	0.67	0.000	0.99	0.36	0.042	2.41	54.02	0.67	0.000	1.49	-0.06	0.745	2.77
7	42.10	0.76	0.000	0.46	0.89	0.000	1.57	26.24	0.83	0.000	0.36	0.72	0.000	1.34
8	58.41	0.38	0.037	0.63	0.50	0.004	2.41	41.62	0.65	0.000	0.36	0.06	0.764	2.36
9	34.18	0.81	0.000	0.46	0.75	0.000	1.61	28.76	0.79	0.000	0.64	0.11	0.566	1.76
10	11.43	0.83	0.000	0.52	0.68	0.000	0.85	13.58	0.88	0.000	0.40	0.74	0.000	0.98
11	25.38	0.63	0.000	0.44	0.69	0.000	1.40	24.76	0.48	0.008	0.83	0.51	0.004	1.36
12	18.33	0.70	0.000	0.66	0.76	0.000	1.17	18.36	0.67	0.000	0.44	0.63	0.000	1.08
13	15.04	0.80	0.000	0.31	0.83	0.000	0.87	15.39	0.85	0.000	0.37	0.48	0.007	1.08
14	29.70	0.55	0.002	0.58	0.67	0.000	1.59	15.37	0.40	0.027	0.37	-0.47	0.008	1.18
15	19.80	0.83	0.000	0.51	0.79	0.000	1.18	26.32	0.20	0.293	0.27	0.71	0.000	1.48
16	24.46	0.82	0.000	0.39	0.86	0.000	1.19	24.42	0.67	0.000	0.49	0.78	0.000	1.46
17	33.30	0.84	0.000	0.59	0.77	0.000	1.50	35.33	0.91	0.000	0.18	0.78	0.000	1.83
18	24.75	0.60	0.000	0.67	0.82	0.000	1.59	31.84	0.71	0.000	0.54	0.45	0.013	1.74
19	25.26	0.92	0.000	0.35	0.92	0.000	1.12	13.92	0.83	0.000	0.36	0.43	0.023	0.87
20	18.56	0.76	0.000	0.29	0.88	0.000	0.99	16.46	0.72	0.000	0.30	0.60	0.001	1.17
21	11.87	0.86	0.000	0.60	0.75	0.000	0.84	13.36	0.82	0.000	0.83	0.57	0.001	1.07
22	18.15	0.79	0.000	0.70	0.88	0.000	1.11	17.43	0.90	0.000	0.75	0.69	0.000	1.23
23	10.40	0.83	0.000	0.53	0.78	0.000	1.00	14.72	0.84	0.000	0.26	0.30	0.114	0.82
Avg.	**24.33**	**0.75**	**0.002**	**0.55**	**0.75**	**0.002**	**1.31**	**21.46**	**0.73**	**0.014**	**0.55**	**0.43**	**0.122**	**1.35**

Supplementary Table 2: Median absolute error and correlation between stimuli and behavioral responses for all participants. Red values are Pearson's-correlation coefficients less than 0.5. The correlation coefficients R can be interpreted as how well the pattern of participant responses match the pattern of stimuli presentation. The errors presented here are the median error (absolute value of response minus stimuli) across all trials. Median error can appear quite high, due to errors on small-magnitude trials. The bolded row at the bottom are the averages for each column.

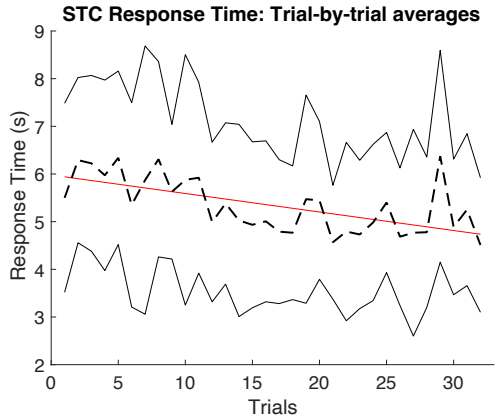

Supplementary Figure 1: Average response time for each trial of the Scalene Triangle Condition. The dotted line is the mean response time, and the upper and lower bounds are 1 standard deviation. There is a slight reduction in response time over the course of the condition. We measured the reduction by fitting a line to the means (red) and looking at the initial value (5.94 sec) and final value (4.74 sec). In this condition, average response time decreased by 1.2 seconds, which is about 20.2% of the initial mean response time.

		Distance r/q	Distance shift (mm)	Angle r/q	Angle Shift Right Turns (radians)	Angle Shift Left Turns (radians)
STC	**EM**	2.32 ± 3.03	-0.16 ± 0.19	1.66 ± 2.71	0.14 ± 0.15	0.11 ± 0.15
	TM	2.29 ± 3.6	-0.38 ± 0.34	2.06 ± 2.92	-0.30 ± 0.36	-0.22 ± 0.38
RTC	**EM**	(from STC)	-0.22 ± 0.15	(from STC)	0.10 ± 0.12	0.10 ± 0.13
	TM	(from STC)	-0.13 ± 0.14	(from STC)	-0.14 ± 0.18	-0.18 ± 0.29

Supplementary Table 3: Mean and standard deviation of model parameters for each model and condition. The r/q parameters are the same between conditions because these parameters were fitted once in the STC and held constant when fitting the shift parameters in the RTC. The fitting was accomplished by minimizing the distance between the Participants' actual final positions and their predicted final position on every trial via the Matlab function lsqnonlin. A lower bound of 0 and an upper bound of 9.07 was used for r/q parameters.

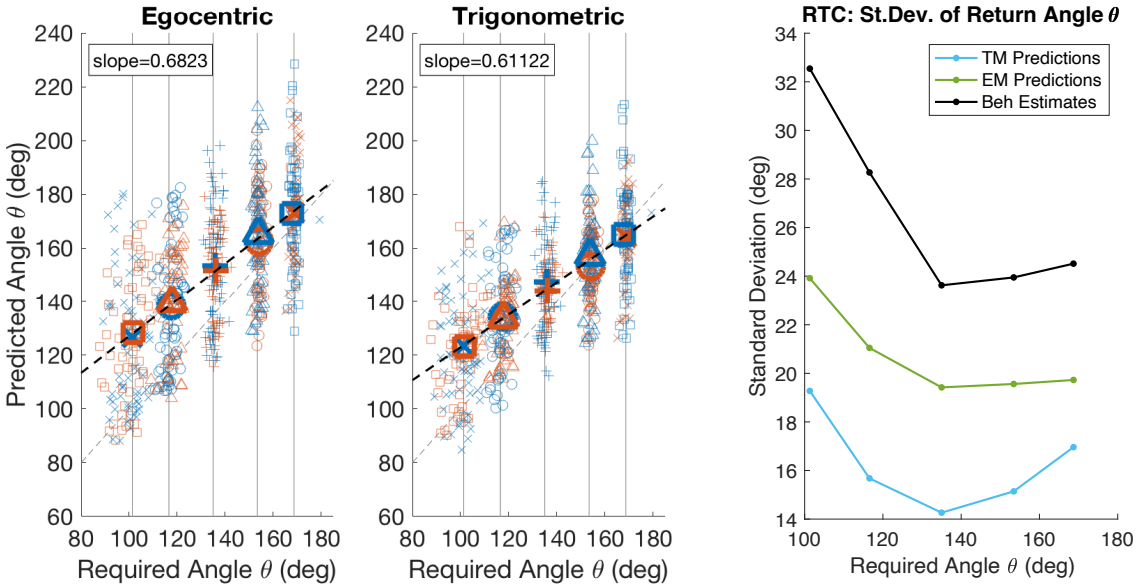

Supplementary Figure 2: Average trends in prediction-vs.-stimuli plots for the RTC. Model predictions from all participants and trials were pooled and segregated based on turn direction (color) and triangle geometry (shape). This plot is intended to be compared to Figure 3. Relevant differences between these two plots include the slope of the fitted lines and the distribution of variance across stimulus angle. When plotting predicted angle against the required homing angle, we see that the EM predictions have a steeper slope than the TM, which is more similar to the slope of the behavioral data (Fig. 3). The standard deviation of the model predictions for each stimulus angle is larger for the EM than the TM, which again is closer to the behavioral data.

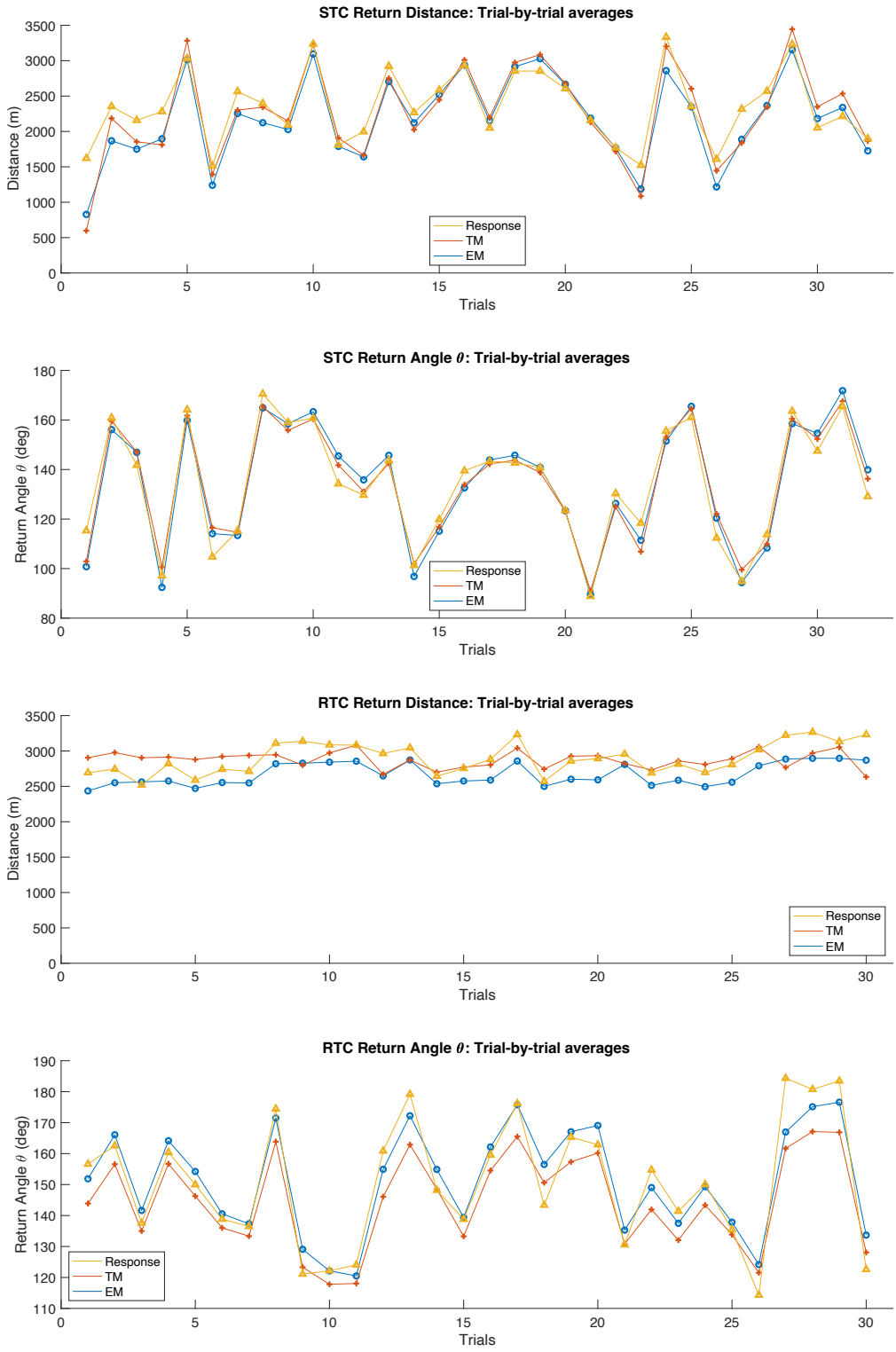

Supplementary Figure 3: Averages across participants for each experimental trail. Top: The average trial-by-trial behavioral responses for return distance in the Scalene Triangle Condition (STC) are plotted above in yellow alongside the average model predictions for each trial across all participants. **Middle-Top:** The average trial-by-trial behavioral responses and model predictions for return angle in the STC. **Middle-Bottom:** The average trial-by-trial behavioral responses for return distance are plotted above in yellow alongside the average model predictions for each trial across all participants in the Right Triangle Condition (RTC). **Bottom:** Average participant responses and model predictions for return angles in the RTC.

CHAPTER 4: Discussion and Conclusions

It is helpful to place the two manuscripts presented here into a context originally published by Wiener et al. in 2010, called the Navigational Toolbox (Wiener et al., 2011). The toolbox is a 4-level hierarchical framework that starts with sensory processes and culminates in high-level navigation constructs like physical maps, wayfinding signage, and human language. At each level of the hierarchy, representations that are meaningful to navigation are constructed from elements in the next lowest level. This thesis' first manuscript contains research on the transition from level 1 to 2: i.e. the formation of "spatial primitives" from elements in the "sensorimotor toolbox." Specifically, we examined the process by which angular distance was derived from measurements of angular velocity provided by endolymph movement through the semicircular canals and movement of the visual environment over the retina. Angular distance and velocity are both spatial primitives that are derived from the vestibular and visual senses.

The research in this thesis' second manuscript concerns elements of level 2 and indirectly the transition from level 2 to level 3 of the Navigational Toolbox, i.e. the derivation of "spatial constructs" from spatial primitives. The process of path integration results in a homing vector that can be used to calculate position. The homing vector is another spatial primitive, but position is a spatial construct because it normally implies one's position in a spatial context, which makes it more meaningful than distance, for example. In the triangle completion experiment, where participants are intentionally disoriented between trials, the participants don't have a spatial context. Also, the participants never need to convert the homing vector to position, because the homing vector alone is sufficient to solve the task. Thus, in most regards the research contained in the second manuscript concerns level 2 of the toolbox. However, many subjects reported that they visualized the triangles from a top-down perspective, e.g. as if they were drawing them on paper. It is unclear if this had any outcomes on their behavior, but cognitive maps are clear examples of spatial constructs.

Bayesian priors for spatial primitives

One way in which the results from the first manuscript bolster the arguments of the second manuscript, is that we provided evidence for the use of a Bayesian prior when representing angular displacement. We found that the

application of a model containing a Bayesian prior for angular displacement accurately predicted reproduction data under conditions when only visual or vestibular sensory information was available, as well as when both were available. It is therefore likely that people are maintaining a Bayesian prior for turned angle and, based on other research, we suspect that Bayesian priors are also maintained for estimated distances (Petzschner & Glasauer, 2011).

The models formulated in the second manuscript depend entirely on the above findings and leverage them to differentiate between the continuous and configural navigation strategies. The meaningful differences between the models' predictions emerge because of the different priors and how they bias estimations of the different geometric elements of the triangles. Obviously, without including priors, the models would be equivalent.

Struggling against sensory noise

Another common theme between the manuscripts is the topic of sensory noise. In the first manuscript we show that our participants were reducing measurement noise by fusing the vestibular and visual sensory inputs. The modeling results confirmed fusion was occurring but indicated that combining two senses via optimal sensory fusion according to MLE often produces only small benefits. Still, other research suggests that the benefits of multimodal integration with two senses extends to the use of even more senses and, mathematically, the benefit of noise reduction should continue to increase with additional sensory inputs (Ernst & Bülthoff, 2004; Jürgens & Becker, 2006; Laurens & Angelaki, 2017). Since we know that measurements of self-rotation under naturalistic conditions use at least 3 senses (visual, vestibular, and proprioceptive) and the motor efference copy, we would expect accuracy above what we demonstrated in the first manuscript. This is primarily because the participants in that experiment rotated themselves via button press and therefore proprioception and efference copies probably contributed very little to sensing the angular displacement. What is undeniable, is that multisensory integration is a very helpful tool for reducing noise at level 1 of the Navigational Toolbox.

The problem of sensory noise is heavily exacerbated in the context of idiothetic path integration during blindfolded navigation, especially for navigators using the continuous strategy. Not only are the number of available senses reduced, but we continuously accumulate error during

measurement and movement. Theoretical evidence suggests that accumulated error is so immense that path integration, without calibrating based on external cues, become completely uninformative past approximately 60 steps (assuming positional updating at each step) (Cheung & Vickerstaff, 2010). This is also supported by experimental evidence which shows that idiothetic path integration by human participants becomes very inaccurate over longer distances (Klatzky et al., 1990). Luckily, this problem can be easily solved using tools from level 3 of the Navigational Toolbox such as external landmarks. The theoretical investigation referenced earlier showed that by using a distal landmark, they could eliminate accumulated error entirely.

Thus, we have methods for reducing sensory noise in level 1 and level 3 of the Navigational Toolbox, but what of level 2? We have, in fact, already heavily discussed a method for reducing noise during measurements of spatial primitives: the Bayesian prior. In situations where the same spatial primitive must be measured many times, let say the distance covered by a single step during unhindered walking, the mean of the Bayesian prior would converge on the average step length. If, for whatever reason, sensory noise was to suddenly increase, the contribution of the prior to estimates of step length would reduce the impact of sensory noise by biasing all measurements of step length towards the mean. Thus, animals possess a variety of compensatory tools that insure accurate measurements and, by extension, accurate navigation.

iPI suffices in bounded environments

Based on the last section, it would seem like idiothetic path integration (iPI) is very limited without regular calibration from external cues. Although, I believe this is generally true, a recent theoretical work by Allen Cheung presents a very interesting exception to this trend. His work suggest that iPI in a familiar bounded area can provide accurate estimates of one's location even over long periods of time, without allothetic cues or knowledge of starting position and orientation (Cheung, 2014). There are only two preconditions: 1) the shape of the arena must possess one-fold rotational symmetry and 2) the navigating agent must know the geometry of the bounded area. Furthermore, the boundaries themselves do not need to be physical barriers, meaning that the navigating agent can create imagined boundaries using landmarks. Thus, a navigating agent could parse a large space into bounded areas that they are familiar with and therefore navigable

using only iPI. Cheung proposes that using only idiothetic cues in a familiar space would free up computational and attentional resources for allothetic processing, which aligns very well with other evidence concerning the automatic nature of path integration (May & Klatzky, 2000). Cheung leaves the question open concerning how the boundary maps would initially be collected, but other theoretical works exist that suggest that path integration could suffice for creating maps as well (Biegler, 2000; Wang, 2016). Therefore, the work contained in this thesis, which provides insights into the cognition related to PI, may help clarify how PI contributes to human navigation more widely.

Concluding remarks

In seeking to understand the role of magnitude estimation in navigation, we started with the fundamental process of measuring our own angular displacement. This spatial primitive enables us to automatically update our orientation in a greater spatial context, and when combined with distance measurements via path integration, we can update our position as well. At both levels of processing, it appears as though people rely upon their prior measurements of distance and angle, to improve their performance and reduce uncertainty. If prior experience does not only influence the spatial primitives of distance and angle, but in fact all spatial primitives, Bayesian modeling can provide a powerful and widely applicable tool for predicting human navigation behavior. Furthermore, the approach presented here may be extended past level 2 of the Navigational Toolbox to predict higher-level navigation behaviors.

References

Aharon, G., Sadot, M., & Yovel, Y. (2017). Bats Use Path Integration Rather Than Acoustic Flow to Assess Flight Distance along Flyways. *Current Biology*, *27*(23), 3650-3657.e3. https://doi.org/10.1016/j.cub.2017.10.012

Alais, D., & Burr, D. (2004). The Ventriloquist Effect Results from Near-Optimal Bimodal Integration. *Current Biology*, *14*(3), 257–262. https://doi.org/10.1016/j.cub.2004.01.029

Apuzen-Ito, G. (2014, November 25). *GG413: Directional Data 1, plotting and computing statistics*. https://youtu.be/J67oydTMwEI?si=RZ4CmlodoNB25J6M

Ashourian, P., & Loewenstein, Y. (2011). Bayesian Inference Underlies the Contraction Bias in Delayed Comparison Tasks. *PLoS ONE*, *6*(5), e19551. https://doi.org/10.1371/journal.pone.0019551

Battaglia, P. W., Jacobs, R. A., & Aslin, R. N. (2003). Bayesian integration of visual and auditory signals for spatial localization. *Journal of the Optical Society of America. A, Optics, Image Science, and Vision*, *20*(7), 1391–1397.

Bear, M. F., Connors, B. W., & Paradiso, M. A. (2007). *Neuroscience: Exploring the brain, 3rd ed.* (pp. xxxviii, 857). Lippincott Williams & Wilkins Publishers.

Bennett, J. (2017). *4. Dead reckoning, longitude, and time* (Vol. 1). Oxford University Press. https://doi.org/10.1093/actrade/9780198733713.003.0004

Biegler, R. (2000). Possible uses of path integration in animal navigation. *Animal Learning & Behavior*, *28*(3), 257–277. https://doi.org/10.3758/BF03200260

Cheung, A. (2014). Estimating Location without External Cues. *PLoS Computational Biology*, *10*(10), e1003927. https://doi.org/10.1371/journal.pcbi.1003927

Cheung, A., & Vickerstaff, R. (2010). Finding the Way with a Noisy Brain. *PLoS Computational Biology*, *6*(11), e1000992. https://doi.org/10.1371/journal.pcbi.1000992

Cheung, A., Zhang, S., Stricker, C., & Srinivasan, M. V. (2007). Animal navigation: The difficulty of moving in a straight line. *Biological Cybernetics*, *97*(1), 47–61. https://doi.org/10.1007/s00422-007-0158-0

Chrastil, E. R., Nicora, G. L., & Huang, A. (2019). Vision and proprioception make equal contributions to path integration in a novel homing task. *Cognition*, *192*, 103998. https://doi.org/10.1016/j.cognition.2019.06.010

Chrastil, E. R., & Warren, W. H. (2017). Rotational error in path integration: Encoding and execution errors in angle reproduction. *Experimental Brain Research*, *235*(6), 1885–1897. https://doi.org/10.1007/s00221-017-4910-y

Cicchini, G. M., Arrighi, R., Cecchetti, L., Giusti, M., & Burr, D. C. (2012). Optimal Encoding of Interval Timing in Expert Percussionists. *Journal of Neuroscience*, *32*(3), 1056–1060. https://doi.org/10.1523/JNEUROSCI.3411-11.2012

Collett, M., & Collett, T. S. (2000). How do insects use path integration for their navigation? *Biological Cybernetics*, *83*(3), 245–259. https://doi.org/10.1007/s004220000168

Collett, T. S. (2019). Path integration: How details of the honeybee waggle dance and the foraging strategies of desert ants might help in understanding its mechanisms. *The Journal of Experimental Biology*, *222*(11), jeb205187. https://doi.org/10.1242/jeb.205187

Colombo, D., Serino, S., Tuena, C., Pedroli, E., Dakanalis, A., Cipresso, P., & Riva, G. (2017). Egocentric and allocentric spatial reference frames in aging: A systematic review.

Neuroscience & Biobehavioral Reviews, *80*, 605–621. https://doi.org/10.1016/j.neubiorev.2017.07.012

Cousins, S., Cutfield, N. J., Kaski, D., Palla, A., Seemungal, B. M., Golding, J. F., Staab, J. P., & Bronstein, A. M. (2014). Visual Dependency and Dizziness after Vestibular Neuritis. *PLoS ONE*, *9*(9), e105426. https://doi.org/10.1371/journal.pone.0105426

Dehaene, S., Izard, V., Spelke, E., & Pica, P. (2008). Log or Linear? Distinct Intuitions of the Number Scale in Western and Amazonian Indigene Cultures. *Science*, *320*(5880), 1217–1220. https://doi.org/10.1126/science.1156540

Durgin, F. H., Akagi, M., Gallistel, C. R., & Haiken, W. (2009). The precision of locomotor odometry in humans. *Experimental Brain Research*, *193*(3), 429–436. https://doi.org/10.1007/s00221-008-1640-1

Ernst, M. O., & Banks, M. S. (2002). Humans integrate visual and haptic information in a statistically optimal fashion. *Nature*, *415*(6870), 429–433. https://doi.org/10.1038/415429a

Ernst, M. O., & Bülthoff, H. H. (2004). Merging the senses into a robust percept. *Trends in Cognitive Sciences*, *8*(4), 162–169. https://doi.org/10.1016/j.tics.2004.02.002

Etienne, A. S., & Jeffery, K. J. (2004). Path integration in mammals. *Hippocampus*, *14*(2), 180–192. https://doi.org/10.1002/hipo.10173

Fraser, P. J. (2006). Review: Depth, navigation and orientation in crabs: Angular acceleration, gravity and hydrostatic pressure sensing during path integration. *Marine and Freshwater Behaviour and Physiology*, *39*(2), 87–97. https://doi.org/10.1080/10236240600708439

Fujita, N., Klatzky, R. L., Loomis, J. M., & Golledge, R. G. (1993). The Encoding-Error Model of Pathway Completion without Vision. *Geographical Analysis*, *25*(4), 295–314. https://doi.org/10.1111/j.1538-4632.1993.tb00300.x

Fujita, N., Loomis, J. M., Klatzky, R. L., & Golledge, R. G. (1990). A Minimal Representation for Dead-Reckoning Navigation: Updating the Homing Vector. *Geographical Analysis*, *22*(4), 324–335. https://doi.org/10.1111/j.1538-4632.1990.tb00214.x

Glasauer, S. (2019). Sequential Bayesian updating as a model for human perception. In *Progress in Brain Research* (Vol. 249, pp. 3–18). Elsevier. https://doi.org/10.1016/bs.pbr.2019.04.025

Glasauer, S., Amorim, M. A., Bloomberg, J. J., Reschke, M. F., Peters, B. T., Smith, S. L., & Berthoz, A. (1995). Spatial orientation during locomation following space flight. *Acta Astronautica*, *36*(8–12), 423–431. https://doi.org/10.1016/0094-5765(95)00127-1

Glasauer, S., Amorim, M.-A., Viaud-Delmon, I., & Berthoz, A. (2002). Differential effects of labyrinthine dysfunction on distance and direction during blindfolded walking of a triangular path. *Experimental Brain Research*, *145*(4), 489–497. https://doi.org/10.1007/s00221-002-1146-1

Glasauer, S., & Shi, Z. (2021). The origin of Vierordt's law: The experimental protocol matters. *PsyCh Journal*, *10*(5), 732–741. https://doi.org/10.1002/pchj.464

Gothard, K. M., Skaggs, W. E., & McNaughton, B. L. (1996). Dynamics of Mismatch Correction in the Hippocampal Ensemble Code for Space: Interaction between Path Integration and Environmental Cues. *The Journal of Neuroscience*, *16*(24), 8027–8040. https://doi.org/10.1523/JNEUROSCI.16-24-08027.1996

Gramann, K., Onton, J., Riccobon, D., Mueller, H. J., Bardins, S., & Makeig, S. (2010). Human Brain Dynamics Accompanying Use of Egocentric and Allocentric Reference Frames during Navigation. *Journal of Cognitive Neuroscience*, *22*(12), 2836–2849. https://doi.org/10.1162/jocn.2009.21369

Griffin, A. S., & Etienne, A. S. (1998). Updating the path integrator through a visual fix. *Psychobiology*, *26*(3), 240–248. https://doi.org/10.3758/BF03330612

Harootonian, S. K., Wilson, R. C., Hejtmánek, L., Ziskin, E. M., & Ekstrom, A. D. (2020). Path integration in large-scale space and with novel geometries: Comparing vector addition and encoding-error models. *PLOS Computational Biology*, *16*(5), e1007489. https://doi.org/10.1371/journal.pcbi.1007489

Heinze, S., Narendra, A., & Cheung, A. (2018). Principles of Insect Path Integration. *Current Biology*, *28*(17), 1043–1058. https://doi.org/10.1016/j.cub.2018.04.058

Helmholtz, H. von. (1867). *Handbuch der physiologischen Optik*. Leopold Voss Leipzig; WorldCat.

Hollingworth, H. L. (1910). The central tendency of judgment. *The Journal of Philosophy, Psychology and Scientific Methods*, *7*(17), 461–469.

Jazayeri, M., & Shadlen, M. N. (2010). Temporal context calibrates interval timing. *Nature Neuroscience*, *13*(8), 1020–1026. https://doi.org/10.1038/nn.2590

Jürgens, R., & Becker, W. (2006). Perception of angular displacement without landmarks: Evidence for Bayesian fusion of vestibular, optokinetic, podokinesthetic, and cognitive information. *Experimental Brain Research*, *174*(3), 528–543. https://doi.org/10.1007/s00221-006-0486-7

Kaliuzhna, M., Prsa, M., Gale, S., Lee, S. J., & Blanke, O. (2015). Learning to integrate contradictory multisensory self-motion cue pairings. *Journal of Vision*, *15*(1), 10–10. https://doi.org/10.1167/15.1.10

Klatzky, R. L. (1998). Allocentric and Egocentric Spatial Representations: Definitions, Distinctions, and Interconnections. In C. Freksa, C. Habel, & K. F. Wender (Eds.), *Spatial Cognition* (Vol. 1404, pp. 1–17). Springer Berlin Heidelberg. https://doi.org/10.1007/3-540-69342-4_1

Klatzky, R. L., Beall, A. C., Loomis, J. M., Golledge, R. G., & Philbeck, J. W. (1999). Human navigation ability: Tests of the encoding-error model of path integration. *Spatial Cognition and Computation*, *1*(1), 31–65. https://doi.org/10.1023/A:1010061313300

Klatzky, R. L., Loomis, J. M., Golledge, R. G., Cicinelli, J. G., Doherty, S., & Pellegrino, J. W. (1990). Acquisition of Route and Survey Knowledge in the Absence of Vision. *Journal of Motor Behavior*, *22*(1), 19–43. https://doi.org/10.1080/00222895.1990.10735500

Laming, D. (1999). Prior expectations in cross-modality matching. *Mathematical Social Sciences*, *38*(3), 343–359. https://doi.org/10.1016/S0165-4896(99)00024-4

Landy, M. S., Maloney, L. T., Johnston, E. B., & Young, M. (1995). Measurement and modeling of depth cue combination: In defense of weak fusion. *Vision Research*, *35*(3), 389–412.

Laurens, J., & Angelaki, D. E. (2017). A unified internal model theory to resolve the paradox of active versus passive self-motion sensation. *eLife*, *6*, e28074. https://doi.org/10.7554/eLife.28074

Loomis, J. M., Klatzky, R. L., Golledge, R. G., Cicinelli, J. G., Pellegrino, J. W., & Fry, P. A. (1993). Nonvisual navigation by blind and sighted: Assessment of path integration ability. *Journal of Experimental Psychology: General*, *122*(1), 73–91. https://doi.org/10.1037/0096-3445.122.1.73

May, M., & Klatzky, R. L. (2000). Path integration while ignoring irrelevant movement. *Journal of Experimental Psychology: Learning, Memory, and Cognition*, *26*(1), 169–186. https://doi.org/10.1037/0278-7393.26.1.169

Mittelstaedt, H., & Mittelstaedt, M.-L. (1982). Homing by Path Integration. In F. Papi & H. G. Wallraff (Eds.), *Avian Navigation* (pp. 290–297). Springer Berlin Heidelberg.

Mittelstaedt, M. L., & Glasauer, S. (1991). *Idiothetic navigation in Gerbils and Humans*.

Moller, P., & Görner, P. (1994). Homing by path integration in the spider Agelena labyrinthica Clerck. *Journal of Comparative Physiology A*, *174*(2). https://doi.org/10.1007/BF00193788

Muller, M., & Wehner, R. (1988). Path integration in desert ants, Cataglyphis fortis. *Proceedings of the National Academy of Sciences*, *85*(14), 5287–5290. https://doi.org/10.1073/pnas.85.14.5287

Müller, M., & Wehner, R. (2010). Path Integration Provides a Scaffold for Landmark Learning in Desert Ants. *Current Biology*, *20*(15), 1368–1371. https://doi.org/10.1016/j.cub.2010.06.035

Murray, M. M., Lewkowicz, D. J., Amedi, A., & Wallace, M. T. (2016). Multisensory Processes: A Balancing Act across the Lifespan. *Trends in Neurosciences*, *39*(8), 567–579. https://doi.org/10.1016/j.tins.2016.05.003

O'Connor, M. R. (2019). *Wayfinding: The science and mystery of how humans navigate the world* (First edition). St. Martin's Press.

Olkkonen, M., McCarthy, P. F., & Allred, S. R. (2014). The central tendency bias in color perception: Effects of internal and external noise. *Journal of Vision*, *14*(11), 5–5. https://doi.org/10.1167/14.11.5

Petzschner, F. H., & Glasauer, S. (2011). Iterative Bayesian Estimation as an Explanation for Range and Regression Effects: A Study on Human Path Integration. *Journal of Neuroscience*, *31*(47), 17220–17229. https://doi.org/10.1523/JNEUROSCI.2028-11.2011

Petzschner, F. H., Glasauer, S., & Stephan, K. E. (2015). A Bayesian perspective on magnitude estimation. *Trends in Cognitive Sciences*, *19*(5), 285–293. https://doi.org/10.1016/j.tics.2015.03.002

Pewsey, A., Neuhäuser, M., & Ruxton, G. D. (2013). *Circular statistics in R* (1. ed). Oxford Univ. Press.

Prsa, M., Gale, S., & Blanke, O. (2012). Self-motion leads to mandatory cue fusion across sensory modalities. *Journal of Neurophysiology*, *108*(8), 2282–2291. https://doi.org/10.1152/jn.00439.2012

Redlick, F. P., Jenkin, M., & Harris, L. R. (2001). Humans can use optic flow to estimate distance of travel. *Vision Research*, *41*(2), 213–219. https://doi.org/10.1016/S0042-6989(00)00243-1

Rescorla, M. (2021). Bayesian modeling of the mind: From norms to neurons. *WIREs Cognitive Science*, *12*(1). https://doi.org/10.1002/wcs.1540

Savelli, F., & Knierim, J. J. (2019). Origin and role of path integration in the cognitive representations of the hippocampus: Computational insights into open questions. *The Journal of Experimental Biology*, *222*(Suppl 1), jeb188912. https://doi.org/10.1242/jeb.188912

Shettleworth, S. J. (2010). *Cognition, evolution, and behavior*. http://www.dawsonera.com/depp/reader/protected/external/AbstractView/S9780199717811

Stackman, R. W., Golob, E. J., Bassett, J. P., & Taube, J. S. (2003). Passive Transport Disrupts Directional Path Integration by Rat Head Direction Cells. *Journal of Neurophysiology*, *90*(5), 2862–2874. https://doi.org/10.1152/jn.00346.2003

Stangl, M., Kanitscheider, I., Riemer, M., Fiete, I., & Wolbers, T. (2020). Sources of path integration error in young and aging humans. *Nature Communications*, *11*(1), 2626. https://doi.org/10.1038/s41467-020-15805-9

Stevens, S. S., & Greenbaum, H. B. (1966). Regression effect in psychophysical judgment. *Perception & Psychophysics*, *1*(5), 439–446. https://doi.org/10.3758/BF03207424

Stocker, A. A., & Simoncelli, E. P. (2006). Noise characteristics and prior expectations in human visual speed perception. *Nature Neuroscience*, *9*(4), 578–585. https://doi.org/10.1038/nn1669

Tsoar, A., Nathan, R., Bartan, Y., Vyssotski, A., Dell'Omo, G., & Ulanovsky, N. (2011). Large-scale navigational map in a mammal. *Proceedings of the National Academy of Sciences*, *108*(37). https://doi.org/10.1073/pnas.1107365108

Tuthill, J. C., & Azim, E. (2018). Proprioception. *Current Biology*, *28*(5), R194–R203. https://doi.org/10.1016/j.cub.2018.01.064

Vilares, I., & Kording, K. (2011). Bayesian models: The structure of the world, uncertainty, behavior, and the brain: Bayesian models and the world. *Annals of the New York Academy of Sciences*, *1224*(1), 22–39. https://doi.org/10.1111/j.1749-6632.2011.05965.x

Wang, R. F. (2016). Building a cognitive map by assembling multiple path integration systems. *Psychonomic Bulletin & Review*, *23*(3), 692–702. https://doi.org/10.3758/s13423-015-0952-y

Wiener, J. M., Berthoz, A., & Wolbers, T. (2010). Dissociable cognitive mechanisms underlying human path integration. *Experimental Brain Research*, *208*(1), 61–71. https://doi.org/10.1007/s00221-010-2460-7

Wiener, J. M., Schettleworth, S., Bingman, V. P., Cheng, K., Healy, S., Jacobs, L., Jeffery, K. J., Mallot, H. A., Menzel, R., & Newcombe, N. S. (2011). Animal Navigation – A Synthesis. In *Animal Thinking: Contemporary Issues in Comparative Cognition* (pp. 51–76). MIT Press.

Wittlinger, M., Wehner, R., & Wolf, H. (2007). The desert ant odometer: A stride integrator that accounts for stride length and walking speed. *Journal of Experimental Biology*, *210*(2), 198–207. https://doi.org/10.1242/jeb.02657

Worchel, P. (1951). Space perception and orientation in the blind. *Psychological Monographs: General and Applied*, *65*(15), i–28. https://doi.org/10.1037/h0093640

Zeil, J., & Layne, J. (2002). Path Integration in Fiddler Crabs and Its Relation to Habitat and Social Life. In K. Wiese (Ed.), *Crustacean Experimental Systems in Neurobiology* (pp. 227–246). Springer Berlin Heidelberg.

Acknowledgments

The work underlying this dissertation was made possible and enlivened by many colleagues, friends, and family, and without them it may not have come to fruition. In particular, I would like to offer gracious thanks to:

My supervisor, Stefan Glasauer, for years of judicious suggestions, guiding advice, and understanding in the face of adverse circumstances.

The administrative faculty of the GSN for their bottomless patience and consistent support.

Kay Thurley, who's amicable critiques brought me clarity and who's supportive words spurred me over a difficult hurdle.

Strongway, who provided an exceptionally thorough and punctual review of the first manuscript in my PhD, in addition to regular feedback in meetings.

Theresa, Alex, and Johanna, who's irreplaceable company made work fun and who's help made my life so much easier.

My father for always being excited about my work, even when I was not.

My mother for encouraging me to achieve my passions and for broadening my horizons.

My wife, Conny, whose strength cleared the way for me to finish this thesis, and whose encouragement repeatedly gave me the push needed to see it through.

Declaration of author contributions

Manuscript
Bayesian priors are maintained for estimated values during continuous and configural navigation strategies

Authors
Joshua W.G. Yudice & Stefan Glasauer

Contributions
JWGY contributed to the design of the experiment, collected data, performed the analysis, and authored the manuscript.
SG contributed to the design of the experiment, provided the computational models, reviewed the manuscript, and contributed to the analysis.

Signatures

Joshua W.G. Yudice Stefan Glasauer

Declaration of author contributions (continued)

Manuscript
Self-rotation perception using visual and vestibular stimuli relies on prior information and sensory fusion

Authors
Joshua W.G. Yudice, Johanna Bayer, Chris J. Bockisch, Juliane Pawlitzki, Zhuanghua Shi, & Stefan Glasauer

Contributions
JWGY collected data, modified the computational models, performed the analysis, and authored the manuscript.
JB contributed to the design of the experiment and collected data.
CJB contributed to the design of the experiment and collected data.
JP contributing by reviewing the manuscript.
ZS contributed to the interpretation of the results and reviewed the manuscript.
SG contributed to the design of the experiment, collected data, provided the computational models, and reviewed the manuscript.

Signatures

Joshua W.G. Yudice Stefan Glasauer